CHAPTER 6

Non-linear Response Dependence on Ground Motion Characteristics with Implications for Ground Motion Record Selection

6.1 Abstract

Ground motion record selection is considered a critical problem in assessment of structural response based on numerical dynamic analysis. The structural engineer expects the ground motion specialist to select records whose magnitudes, distances, site conditions, and faulting style are representative of the threat to the site. This may be accomplished with the use of "disaggregation" (see McGuire, 1995). In some cases the records are selected to provide response spectra that approximate the uniform hazard spectrum or other "design" response spectrum. The properties (natural period, etc) of the structure may or may not be considered in the record selection. The choice of the ground motions may be affected by the interface variable used to measure the intensity of ground motion, known in PEER as the intensity measure IM. According to criteria proposed by Luco and Cornell (2001), a preferred IM is both "sufficient" with respect to the ground motion characteristics and also "efficient". A sufficient intensity measure renders the structural response conditionally statistically independent of other ground motion characteristics such as event magnitude, while an efficient intensity measure predicts the structural response with (relatively) small record-to-record variability. Theoretically, careful record selection is not essential if the intensity measure is demonstrated to be sufficient with respect to ground motion characteristics.

The spectral acceleration of the first-mode frequency (FMF) is commonly used as a scalar-based intensity measure in probabilistic seismic assessments. Shome and Cornell (1999) have demonstrated that spectral acceleration at FMF is sufficient with respect to the ground motion characteristics for moment resisting frame structures with FMF's in the moderate period range. In this study, the nonlinear dynamic displacement responses of two extreme cases of short-period SDOF and long-period MDOF structural systems are presented. The short period system is a generic SDOF bi-linear model with T=0.1 sec; and the long-period system is a 20 story moment-resisting steel frame structure (LA 20 structure, see Luco, 1999) with T_1=3.98 sec. For both cases,

it is demonstrated that the FMF spectral acceleration renders the maximum inter-story drift response effectively conditionally independent of ground motion characteristics such as magnitude, source-to-site distance, and normalized residual (epsilon) of the attenuation relationship.

It is of interest to investigate the sufficiency of the FMF spectral acceleration over a range of ductility levels and hence nonlinear behavior. Therefore, the yield strength level for the SDOF system is adjusted in order to achieve structural response in a desired range of ductility. It is demonstrated that the FMF spectral acceleration is also sufficient for the SDOF system with modified yield strength and hence ductility level of the response. As an alternative to adjusting the yield strength in the case of the SDOF system, the 20-story structure is subjected to ground motion records that are scaled so that they render the structural response in a desired range of ductility. It is also demonstrated that the FMF spectral acceleration is effectively sufficient based on the response of the 20-story structure to the scaled ground motion records. These studies suggest that the sufficiency of the FMF spectral acceleration is maintained at various levels of linear and non-linear response and ductility.

For these two systems this sufficiency conclusion is not necessarily to be expected. Their non-linear responses are expected to be particularly spectral shape sensitive and that shape is thought to be magnitude dependent. Therefore, response is expected to be magnitude dependent. This logic is studied step-by-step. For both example cases, dependence of the response, once it is conditioned on the FMF spectral acceleration, on the shape of the elastic response spectrum is investigated. The effect of the shape of the spectrum is measured by the spectral acceleration at period T normalized to the FMF spectral acceleration, also known as the spectral shape factor at period T. This is equivalent to measuring the relative efficiency of a vector-based intensity measure consisting of FMF spectral acceleration and spectral shape factor at period T. In the case of the 20 story structure (with long period), the response demonstrates significant dependence on the spectral shape factor at a period close to the second mode frequency (SMF). In the case of the SDOF system (with short period), the response is significantly dependent on the spectral shape factor at a period larger than (about two to three times) the period at FMF. These observations are confirmed for different ductility ranges by studying SDOF systems with varying yield strength and by scaling the ground motion records in the case of the LA20 structure.

On the other hand, it is expected that the spectral shape factor demonstrate magnitude-dependence. This hypothesis is investigated based both on the attenuation predictions for the shape factor as a function of magnitude and also on the relation between magnitude and the spectral shape factor of the ground motions used in this study. As stated above, if the shape-factor is magnitude dependent, one would expect that the structural response conditioned on the FMF spectral acceleration be also dependent on magnitude. This would explain why ground motion magnitude is conceived as the most likely ground motion variable to affect the structural response conditioned on the FMF spectral acceleration. However, the established sufficiency of the FMF spectral acceleration with respect to magnitude seems to contradict such presumptions. It is argued that the large variability in both the relation of response to shape factor and also the relation of spectral shape to magnitude may explain the observed lack of conditional dependence on ground motion magnitude.

The sufficiency found here will not necessarily carry over to all cases. Sufficiency depends on the IM, the structure, the response, and the ground motion parameters. Ground motion parameters such as site amplification and/or directivity may prove particularly troublesome because they may imply strong sensitivity of spectral shape to certain ground motion parameters (impedance ratio, "$X \cdot \cos(\theta)$,M, etc.). If for a specific structure, the proposed intensity measure is not sufficient with respect to ground motion characteristics, it will be argued that the results of probabilistic seismic hazard analysis (specifically via site-specific seismic hazard disaggregation) can be used to appropriately adjust the response statistics for a given selection of records to correct for possible dependencies on ground motion characteristics, at least within certain limitations.

6.2 Keywords

Intensity measure, probabilistic seismic hazard analysis, moment magnitude, nonlinear dynamic analysis, attenuation relationships, scaling, ground motion record selection

6.3 Introduction

The probabilistic seismic assessment of structures normally requires performing a set of time-history analyses on a suite of ground motion records. This will provide an estimate of the central value and the variability in structural response under seismic excitations. The estimated distribution of structural response is dependent on the suite of ground motions used for the time-history analyses. Ideally, these ground motions should represent the major earthquake scenarios

that can happen for a particular site condition. However, finding a selection of records that represents all the possible earthquake scenarios and their relative likelihood for a site can be extremely cumbersome; in fact it is not quite clear precisely what a "representative record selection" is and in any case it may change with return period or IM level. Nevertheless, depending on the performance level under consideration, only a subset of the possible earthquake scenarios are going to be significant in terms of the probability of their occurrence. If the significance of scenario earthquakes for a given performance level is measured by probabilistic criteria, an efficient record selection would consist of choosing records representing those scenario events with the largest relative contribution to the probability of exceedance (hazard) corresponding to that performance level. This objective is approximated in some current practice by disaggregation of spectral acceleration hazard with respect to M, R_{rup} (see Somerville et al., 1998 and Stewart et al. 2001). On the other hand, the statistical properties of structural response to a given selection of records can be adjusted by weighting the response based on the actual (relative) contribution of each record to the hazard corresponding to a particular performance level.

The strength of ground motion is represented by a variable called the intensity measure in the certain current earthquake engineering literature. The intensity measure IM serves as an interface variable that implicitly represents the ground motion characteristics such as magnitude and distance in the seismic assessment of a structure. Most common choices for the intensity measure are the peak ground acceleration (PGA) and the spectral acceleration for a specified oscillator frequency and damping. Luco and Cornell (2001) proposed probability-based and structure-specific criteria for the selection of the ground motion intensity measure variable. These criteria gauge the success of a candidate intensity measure in terms of how small the bias and variability in the resulting structural response is going to be. According to these criteria, a preferred candidate for the intensity is both "efficient" and "sufficient" with respect to the selected structural response variable. An "efficient" intensity measure results in relatively small variability in the structural response; while the "sufficient" intensity measure renders the response conditionally statistically independent of the ground motion characteristics. It will be demonstrated that the criteria for record selection will be significantly simplified when the selected intensity measure is sufficient with respect to the structural response variable.

This chapter demonstrates how sufficiency of FMF spectral acceleration with respect to ground motion characteristics can be established based on a suite of ground motion records. Shome and

Cornell (1999) have demonstrated that the FMF spectral acceleration is sufficient with respect to ground motion characteristics for first-mode dominated moment resisting frame structures with moderate FMF's. Hence, this chapter focuses on structures with extreme FMF's and on structures where the second-mode is expected to be important. As example cases, the sufficiency of spectral acceleration is investigated for two structures, a 20-story steel moment-resisting frame with $T_1 = 3.98$, and a generic SDOF system with $T = 0.1$. For these example cases, the sufficiency of FMF spectral acceleration is investigated based on "un-scaled" ground motion records. In addition to the ground motion characteristics, the dependence of the response on the shape of the elastic acceleration spectrum is also investigated. It is demonstrated that the structural response conditioned on the FMF spectral acceleration (also a measure of the amplitude of the spectrum at FMF) is dependent on the shape of the spectrum. The effect of the shape of the spectrum is measured by the spectral acceleration at period T normalized by the FMF spectral acceleration, $S_a(T)/S_a(T_{FM})$, also known as the spectral shape factor at period T. For the 20-story structure, the displacement-based response of the structure is expected to exhibit second-mode dependence, where as for the high-frequency SDOF system, the displacement-based non-linear response is expected to exhibit dependence on the spectral shape at frequencies smaller than FMF. Hence for both cases, the displacement-based response is expected to depend on the spectral shape factor at a period T different from T_{FM}.

It will also be demonstrated that the spectral shape factor at a period T may demonstrate some degree of dependence on the moment magnitude. Such dependence is studied both from the point of view of the attenuation predictions for spectral shape as a function of magnitude and also from the observed relation between spectral shape and magnitude for the suite of records used in this study. The dependence of the displacement-based response on the spectral shape factor together with the dependence of the spectral shape factor on magnitude suggest that the displacement-based response may in turn exhibit dependence on moment magnitude. This hypothesis is a basis for expecting that the moment magnitude be the most likely ground motion characteristic variable to be correlated to the structural displacement response conditioned on $S_a(T_{FM})$. Such hypothesis is investigated in detail for both structural systems as part of the sufficiency investigations.

A suite of simple linear regressions together with tests of hypotheses is used for evaluating the sufficiency of $S_a(T_{FM})$ with respect to ground motion characteristics and also measuring the dependence of the response on the shape of the spectrum. However, a more thorough

investigation may use multiple-variable regression for investigating the sufficiency of $S_a(T_{FM})$ with respect to ground motion characteristic variables M and R_{rup}, ε simultaneously.

In order to investigate the sufficiency of $S_a(T_{FM})$ for higher ductility levels, the ground motion records are scaled by a factor of three in the 20-story example case. For the SDOF structure, the sufficiency of $S_a(T_{FM})$ is investigated for different ductility levels, by varying the yield strength. In both cases, it is observed that the sufficiency of $S_a(T_{FM})$ is maintained over a broad range of non-linear behavior and ductility. However, this conclusion may not always be true.

Once it is demonstrated how to establish sufficiency for a scalar *IM*, the advantages of a choosing a sufficient intensity measure are discussed. It is argued that more-or-less arbitrary selection of record is justified, if the intensity measure is sufficient with respect to those ground motion characteristics that may affect the response.

What happens if sufficiency is not established? The last sections of the chapter focus on cases where the intensity measure is not sufficient. This chapter demonstrates that the response statistics can be adjusted in order to take into account possible dependencies on ground motion characteristics. A procedure for post-processing the structural response based on available hazard disaggregation (see Bazzurro and Cornell 1999) results is presented. This procedure uses the disaggregation results as weights in order to re-adjust the structural response in order to take into account dependencies on ground motion characteristics.

6.4 Records used in this chapter

In the study that follows 47 horizontal ground motion records have been extracted from the PEER strong motion database. The records are all California earthquakes recorded on deep soil (Geomatrix soil types C and D). There have been no particular criteria in choosing the records apart from avoiding the recordings with potential near-sources effects (e.g., directivity) in them. The selected records have magnitudes between 5 and 7.5 and the source-to-site distance from 15 km to 120 km. A complete list of the ground motion records and their characteristics can be found in Appendix C. We will refer to this selection of records as “combined selection”, since it is in fact the combination of the set of 30 ground motions used in Chapters 4 and 5 and another 17 ground motions. The reason for adding the extra 17 ground motions was to increase the range of

the corresponding magnitude values, and hence to make the selection more suitable for studying possible dependencies on ground motion magnitude, i.e., for studying sufficiency.

6.5 Ground motion characteristics

The spectral acceleration at the period T, $S_a(T)$, can be uniquely determined in terms of what shall be called the ground motion characteristics: magnitude *M*, source-to-site distance R_{rup}, and a normalized regression residual, ε, by an attenuation relationship:

$$\ln S_a(T) = f(M, R_{rup}) + \sigma_{\ln S_a} \cdot \varepsilon \qquad (6\text{-}1)$$

where $f(M, R_{rup})$ is a function that produces the median (more precisely, expected value of the log) of all records for the scenario earthquake M and R_{rup} and it referred to as the attenuation law. It is typically obtained by regression. ε is the residual of the attenuation law regression normalized with respect to the dispersion in the attenuation law prediction, $\sigma_{\ln S_a}$. It should be noted that the dispersion in the attenuation law may also depend on the ground motion characteristics. This normalized residual is widely known as the "epsilon" of the attenuation law in the literature. In this study, possible dependencies with respect to the following three ground motion characteristics, magnitude *M*, closest (source-to-site) distance R_{rup}, and the epsilon (the normalized attenuation residual), ε, are going to be investigated.

6.6 The spectral acceleration and the spectral shape factor

It is going to be demonstrated in this study that given the FMF spectral acceleration, the displacement-based response of the structure is dependent on the shape of the elastic acceleration spectrum. The spectral acceleration at a period other than FMF is usually normalized with respect to $S_a(T_{FM})$ in order to reflect the "shape" of the spectrum. Hence, the spectral shape factor at the period, *T*, is denoted by, $R(T, T_{FM})$ and is defined as the ratio of the spectral acceleration at period T to the FMF spectral acceleration:

$$R(T, T_{FM}) = \frac{S_a(T)}{S_a(T_{FM})}$$

The spectral shape factor can be used to demonstrate that the displacement-based response of the structure for a given $S_a(T_{FM})$ depends on the shape of the acceleration spectrum. This together with the possible dependence of spectral shape on magnitude (discussed later in this chapter) would seem to imply that the displacement-based response of the structure given $S_a(T_{FM})$ is also dependent on magnitude.

From a different point of view, it can be argued that the spectral acceleration values at periods other than the FMF may also contain ground motion characteristic information that is not already relayed by $S_a(T_{FM})$. Hence, if they are paired with $S_a(T_{FM})$, the ensemble may better describe the record-to-record variability in the displacement response of the structure (the efficiency criterion). Therefore, establishing the dependence of the structural response given $S_a(T_{FM})$ on the spectral shape factor is equivalent to establishing that the pair of $S_a(T_{FM})$ and $R(T, T_{FM})$ as a vector-valued intensity measure is more "efficient" than $S_a(T_{FM})$ only.

6.7 Maximum inter-story drift angle: The displacement-based response parameter

In this study, the efficiency and sufficiency criteria are investigated based on the predictions for the non-linear dynamic displacement response of the structure, provided by the candidate intensity measure. Hence, establishing the efficiency and sufficiency criteria is dependent on the choice of both the intensity measure and the structural response variable. Maximum inter-story drift angle denoted by $\theta_{\max}$ is chosen as such dynamic displacement-based response variable. For a moment-resisting frame structure, $\theta_{\max}$ is a global response parameter that may reflect the most severe damage incurred by non-linear deformations in the moment connections. Since $\theta_{\max}$ is the response parameter predicted by the intensity measure, it may also be referred to (later in this chapter) as the "dependent variable", wherever linear regression is used to make such predictions.

6.8 Residual-residual plot: A graphical method for measuring the significance of an additional regression variable in predicting the structural response

Linear regression is a useful statistical tool for investigating efficiency and sufficiency criteria for a candidate intensity measure (see Shome and Cornell 1999, and Luco, 2002). The displacement-based response parameter, $\theta_{\max}$, can be predicated as a function of the candidate intensity measure, e.g., $S_a(T_{FM})$, by performing linear regression (usually in the logarithmic scale). The efficiency of the candidate IM can be measured by the variability in the residuals of the regression analysis. In order to establish sufficiency, the effectiveness of ground motion characteristic variables as additional regression variables, i.e., in addition to $S_a(T_{FM})$, can be investigated. In other words, ground motion characteristic variables cause very little improvement in the regression prediction as regression variables in addition to a "sufficient" intensity measure. This improvement may be judged by the reduction in the dispersion of the regression residuals and/or the statistical significance of the regression coefficients corresponding to the ground motion characteristic variables.

In this chapter, a simplified statistical approach based on regression is implemented for measuring the effectiveness of ground motion characteristics as additional regression variables. This method uses a graphical statistical tool known as the residual-residual plot. The main advantage of the residual-residual plots is that they offer visual means for judging the improvement caused by an additional regression variable.

Residual-residual plots are used in the applied statistics in order to investigate whether adding a second variable to the regression improves the predictions compared to predictions based on the regression on the first variable only. These plots are constructed by: a) performing regression of the dependent variable (e.g., the displacement-based response, $\theta_{\max}$) versus the (first) independent variable (e.g., $S_a(T_{FM})$) b) performing regression of the second independent variable (e.g., one of the ground motion characteristics) on also the first variable ($S_a(T_{FM})$) c) plotting the residuals of the two regressions mentioned above against each other.

Roughly speaking, the two regressions on the first variable "eliminate" possible dependence of both the dependent variable ($\theta_{\max}$) and the second independent variable (one of the ground motion characteristics) on the first independent variable ($S_a(T_{FM})$). This facilitates investigating

the potential dependence of the dependent variable on the second variable, by observing a (statistically) significant trend, in the residual-residual plot, between the two sets of residuals explained above. In order to simplify future references to these residuals, the residuals of the regression of the dependent variable on the first variable are also called the "response residuals", and the residual of the regression of the second variable on the first variable are also called the "second-variable residuals". The possible trend between the two sets of residuals may be observed by performing linear regression of "response residuals" on "second variable residuals". The significance of the trend measured by both the variability in the residuals of such regression and/or testing the following hypothesis: *"The slope of the regression line is zero"* (i.e., test of hypothesis, see Rice 1995). The significance of the slope is usually measured by a quantity known as the *p-value*, assuming that the slope of the regression line is a random variable described by *Student's t-distribution* (see Rice 1995). The hypothesis is rejected (i.e., the slope is non-zero) if the *p-value* is smaller than a certain (small) value, e.g., 0.01. If a two-variable regression of the response on both the first and the second independent variable is performed, it can be shown that the regression coefficient for the second variable is going to be the same as the slope of the (simple) regression of the "response residuals" on "second-variable residuals". Moreover, the results of the hypothesis test are going to be identical.

As it is mentioned above, one way to measure the significance of an additional regression variable is by measuring the amount of reduction it causes in the variability of data around the regression prediction. The variability of data around the regression line can be estimated by the (square) root of the mean of squares (RMS) of regression residuals, which is also referred to as the "sigma" of the regression. It should be noted that the "sigma" of the residual-residual regression is the same as that of the two-variable regression of response (dependent variable) on the two independent variables, i.e., the two approaches are equivalent. The smaller is the ratio of the sigma of the residual-residual regression (explained above) to the sigma of the regression of dependent variable on the first variable (or "original" regression for brevity), the more significant is the role of the second regression variable. In simple terms, an effective second regression variable is going to "explain" part of the variability in the data that is not captured by the first regression variable. In the context of sufficiency, this means that if the sigma of the residual-residual regression is (significantly) smaller than the sigma of the original regression, this will also confirm (in addition to the test of hypothesis) that the intensity measure is not sufficient with respect to the ground motion characteristic in question. It also indicates that the two regression variables together can provide a more "efficient" prediction of response, recalling that the

efficiency criterion is based on the variability of response for a given value of the intensity measure.

The residual-residual plots and the test of hypothesis can also be used to as a visual way to establish the sufficiency of $S_a(T_{FM})$ with respect to ground motion characteristics. If the *p-value* for the slope of the regression line on the residual-residual plot is near zero, it can be concluded that $S_a(T_{FM})$ is <u>not</u> sufficient with respect to the particular ground motion characteristic in question. However, it should be noted that in this (simplified) approach the sufficiency of $S_a(T_{FM})$ is questioned for one ground motion characteristic at the time. This would ignore possible interactions between the ground motion characteristics themselves. A more thorough approach consists of performing a multi-variable regression of the displacement-based response (the dependent variable) on $S_a(T_{FM})$ and all of the ground motion characteristics in question, and test the (joint) hypothesis of whether all the regression coefficients corresponding to the ground motion characteristics are simultaneously zero. Nevertheless, it is believed that the residual-residual plot approach is still effective in un-covering potential dependencies of response on ground motion characteristics.

Residual-residual plots are also used in order to establish that the displacement-based response given $S_a(T_{FM})$ depends on the spectral shape factor $R(T,T_{FM})$. In this case, $R(T,T_{FM})$ is the additional regression independent variable whose effectiveness is studied. This is equivalent to maintaining that the vector-valued intensity measure consisting of the two elements, $S_a(T_{FM})$ and $R(T,FM)$, is more "efficient" than the scalar intensity measure $S_a(T_{FM})$. The reduction in the sigma of the residual-residual regression compared to the sigma of the "original" regression in this case reflects the relative efficiency of the pair $S_a(T_{FM})$ and $R(T,T_{FM})$.

6.9 Establishing the sufficiency of $S_a(T_{FMF})$ based on the un-scaled set of records

In this section, the residual-residual plots and hypothesis testing are used in order to investigate the sufficiency of the scalar IM, $S_a(T_{FM})$ with respect to ground motion characteristics.

The observations in this section are based on the ground motion records described in Section 6.4 and Appendix C. Two example cases are discussed. The first example is a 20-story steel moment

resisting frame with a long period ($T_1 = 3.98$ sec). The second example is a generic single-degree-of-freedom system with a very short period ($T = 0.1$ sec). These cases represent structural systems with extreme FMF values, and hence with potential for demonstrating dependencies on ground motion characteristics. For the 20-story structure, the displacement-based response of the structure is expected to be second-mode dependent, where as for the high-frequency SDOF system, the displacement based response is expected to exhibit dependence on the frequencies smaller than FMF (e.g., due to period elongation). For both cases, the dependence of the response on frequencies other than FMF is demonstrated by investigating the dependence of the response on the spectral shape factor at a period T, after it is conditioned on $S_a(T_{FM})$. It is also demonstrated that the shape of the acceleration spectrum depends on the moment magnitude of the ground motion. This explains why the moment magnitude is a likely ground motion characteristic variable to affect the displacement-based response after it is conditioned on $S_a(T_{FM})$.

6.9.1 System with long first-mode period: LA 20 story Results

The 20 story ductile M1+building model used by Luco for near-source studies (Luco and Cornell, 2002) is a good example of a structure whose linear and non-linear dynamic behavior (as measured by maximum inter-story drift ratio) is significantly influenced by higher modes. Therefore spectral shape and magnitude can be expected to affect its response.

The 20-story steel moment resisting frame (SMRF) building was designed for Los Angeles conditions as a part of the SAC steel project (Phase II), according to pre-Northridge earthquakes provisions (see Luco, 2002). The structure is modeled using DRAIN-2DX and is denoted by ductile M1+ in Luco's thesis (2002). The beam-columns are modeled by a bi-linear hysteretic model (DRAIN-2DX, Element 02). This modeled is denoted by M1+ because the effect of the interior gravity frames is considered by linking an equivalent gravity column to the two-dimensional model of the perimeter frame. The p-delta effect is also considered in the analysis of the frame.

Table 6-1 shows the periods corresponding to the first 5 mode shapes for the 20 story frame structure. The spectral acceleration for T=3.9 seconds (close to T_{FM} for the structure) and damping of 5%, is chosen as the $S_a(T_{FM})$.

Mode Number	1	2	3	4	5
Period	3.96	1.35	0.78	0.55	0.41

Table 6-1- Modal periods for LA 20 M1+ model structure

The dynamic displacement response of the structure to ground motion records described in Section 6.4, represented by maximum inter-story angle, $\theta_{\max}$, is plotted in Figure 6-1 versus $S_a(T_{FM})$ on logarithmic paper. The linear regression prediction for $\ln \theta_{\max}$ as a function of $\ln S_a(T_{FM})$ is also plotted (the straight line in the two-way logarithmic plot). As mentioned in Section 6.8, the regression of $\theta_{\max}$ on $S_a(T_{FM})$ is labeled here as the "original regression", as it provides the basis for future comparisons when additional variables are used in order to make predictions. (In this sentence and subsequently the fact that the (linear) regressions are on the logarithm of the variables will be suppressed fro simplicity. The only exception is that magnitude , not logarithm of magnitude is used in the linear regressions.)

It should be noted that the regression of $\ln \theta_{\max}$ on $\ln S_a(T_{FM})$ in the logarithmic scale is equivalent to fitting a power-law function in the form of, $a \cdot S_a^{\ b}$, to the maximum inter-story drift angle data. It should be noted that b=1 corresponds to a linear relationship. This steel moment-resisting frame is expected to behave linearly for maximum inter-story drifts less than about %1. The value reported on the graph as, $\sigma_{\ln \theta_{\max}|S_a} = 0.40$, is the (square) root of the mean squares (RMS) of the residuals of the original regression (often called the standard error of regression), also referred to as the "sigma" of the regression. This value, which is a measure of the dispersion of the displacement response around the linear regression predictions (a straight line in the logarithmic scale), is the basis of later comparisons when additional variables are involved in the predictions. It should be noted that the displacement-based response is plotted on the horizontal axis, as it is conventional in structural engineering. However the displacement-based response is the dependent variable in the regression.

The residual-residual plots, introduced in Section 6.8, are used here in order to investigate the sufficiency of the $S_a(T_{FM})$ with respect to three ground motion characteristics, moment magnitude M, rupture distance (horizontal distance to the projection of the rupture) R_{rup}, and the epsilon (normalized residual of the attenuation relation), ε. For each ground motion characteristic under consideration, the residuals of its regression on $S_a(T_{FM})$ are going to be the

ordinates of points on the residual-residual plot. The abscissas, which are invariable with respect to ground notion characteristic under consideration, are the residuals of the "original" regression of the maximum inter-story drift (the displacement response) $\theta_{\max}$ on $S_a(T_{FM})$.

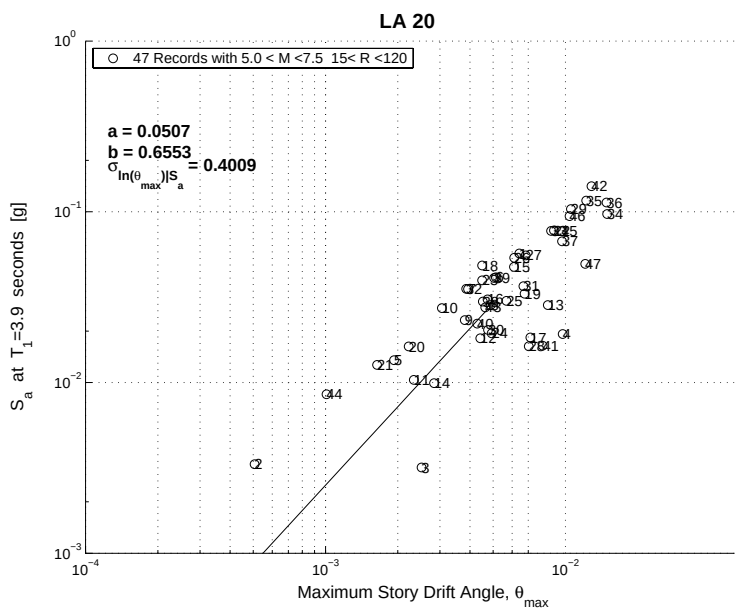

Figure 6-1 - The dynamic displacement response of LA20 model structure to the combined record selection plotted versus the spectral acceleration for T=3.9 sec and %5 damping, $S_a(T_{FM})$

If a (statistically) significant trend is observed between the two residuals on the residual-residual plot, it can be concluded that $S_a(T_{FM})$ is not sufficient with respect to the ground motion characteristic under consideration. In order to measure the possible trend between the two sets of residuals, a line is fit to the points on the plot using simple linear regression.. This is based on a property of linear regression in which the regression prediction passes through the average values of the two sets of horizontal and vertical components. As the two sets of components constructing a residual-residual plot are themselves residuals of linear regressions, their corresponding average values are always equal to zero, and hence the reason why the regression line always passes through the origin. The slope of the regression line, if "significantly" different from zero, indicates and measures the potential trend;. As mentioned in Section 6.8, the test of hypothesis based on the Student-t Distribution is used to test if the slope is "significantly" different from zero. It should be noted that there is a difference between the "strength" of the trend and the "significance" of the trend. While the significance of a trend is measured by the *p-value*, the strength of a trend is measured by the slope of the regression prediction line.

Figure 6-2 is an example of a residual-residual plot used to investigate the significance of rupture distance R_{rup} as a second variable in the regression (consistent with the original regressions and plots, however, a log scale is retained. Hence 10^0 corresponds to a log residual of zero). The *a* value reported on the graph is the intercept of the fitted line. As it is explained above the *a* value is always equal to zero or an infinitesimal number as it is reported on the graph. The *b* value is the slope of the fitted line which is very close to zero in this case (Figure 6-2). The dispersion measure denoted by $\sigma_{\ln residual|\ln residual2}$ is the (square) RMS of the regression residuals. $\sigma_{\ln residual|\ln residual2}$ is a measure of the conditional dispersion of $\ln\theta_{\max}$ given $S_a(T_{FM})$ and the second regression variable (here, the rupture distance, $\ln R_{rup}$). Theoretically speaking, it should be close to or smaller than the conditional dispersion of $\ln\theta_{\max}$ given $S_a(T_{FM})$ only. This means the value for $\sigma_{\ln residual|\ln residual2}$ should be close to or smaller than the value reported for the "original" regression in Figure 6-1 ($\beta_{\theta_{\max}|S_a} = 0.40$). As will be observed in the following residual-residual plots, the value for dispersion is very close to 0.4 in the cases where no trend is observed. This confirms that the second variable is not significant in reducing the dispersion in the regression or in simple words reducing the fraction of the variability in the structural response that is not already explained by $S_a(T_{FM})$. On the contrary, when a significant trend is observed, the reported regression value is (significantly) smaller than $\sigma_{\ln\theta_{\max}|S_a} = 0.40$. The one-sided *p-value* reported on the graph is a measure of the significance of the slope. It is called one-sided because it is a probabilistic measure of how many standard deviations, σ_b, the (absolute value of) slope *b* is <u>greater</u> than zero.

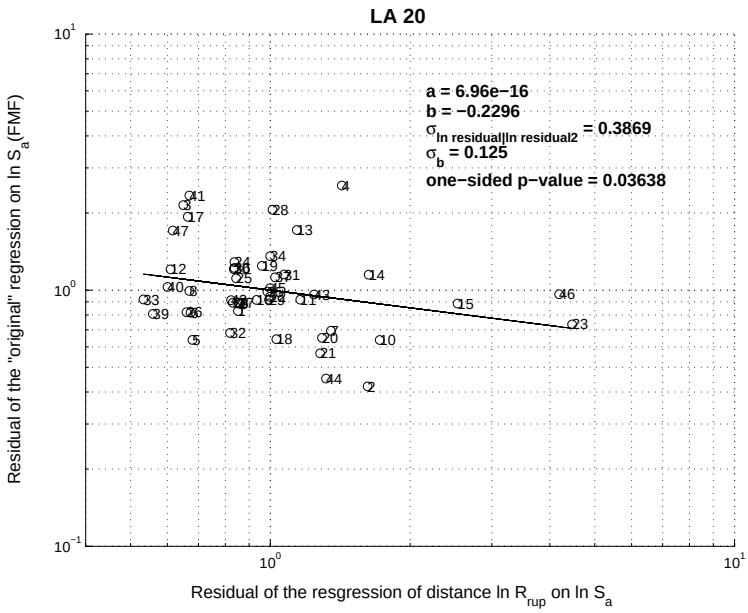

Figure 6-2 - Residual-residual plot for rupture distance, as a second independent variable for predicting structural response for LA20 structure, combined record selection

The value for σ_b is also reported on the graph. If the standard deviation σ_b is very large relative to the slope itself, the slope may not be statistically different from zero. The *p-value* is a probabilistic way of quantifying the above statement. A *p-value* equal or close to zero indicates that the slope is significantly different from zero. Looking at Figure 6-2, it can be observed that there is a weak negative correlation between the two residuals. The p-value reported on the plot is small (%3) but not infinitesimal, which confirms a the existence of a weak trend. However, The dispersion value $\sigma_{\ln residual|\ln residual2}$ is equal to 0.39, which is very close to $\sigma_{\ln\theta_{\max}|S_a} = 0.4$. The negligible reduction in the dispersion indicates that $S_a(T_{FM})$ is "effectively" sufficient with respect to R_{rup}.

The residual-residual plot in Figure 6-3 investigates the sufficiency of $\ln S_a(T_{FM})$ with respect to magnitude, M. As it is explained above, the residuals of the regression of $\ln\theta_{\max}$ and of M on $\ln S_a(T_{FM})$ are plotted against each other. The slope of the fitted line or the *b* value (*b=-0.10*) is slightly less than zero indicating a potential weak dependence. But the *p-value* is not negligible, which means that the reported slope is not significantly different from zero. Also the fact that the reported dispersion, $\sigma_{\ln residual|residual2} \approx 0.40$ is very close to $\sigma_{\ln\theta_{\max}|S_a} = 0.40$ confirms that

magnitude is not significant as a potential second regression variable. As a result, S_a is also sufficient with respect to ground motion magnitude.

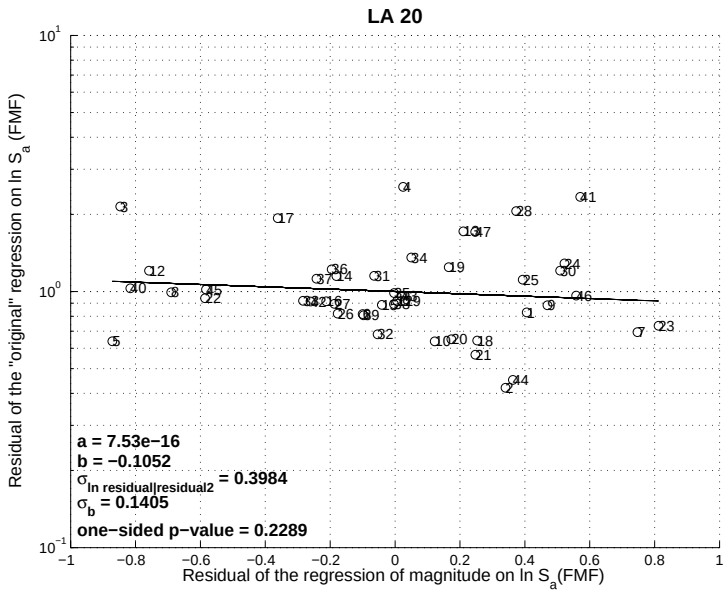

Figure 6-3 - Residual-residual plot for magnitude as a second independent variable for predicting the structural response for LA20 structure, combined record selection

Figure 6-4 investigates the sufficiency of $S_a(T_{FM})$ with respect to the normalized residual (epsilon) of the attenuation law, denoted by ε. The ε values are calculated by finding the attenuation law prediction for the natural logarithm (ln) of spectral acceleration values at T=4 seconds (Equation 6-1), which is close to the FMF for the structure with T_1=3.96 seconds, and subtracting the attenuation predictions from the corresponding ln(spectral acceleration) value for each ground motion record. The attenuation epsilon accounts for any other ground motion characteristic that is not explained by M and R_{rup}. There is no significant trend observed in the residual-residual plot of Figure 6-3. As with the previous plots, the *p-value* is not significant and the sigma of the residual-residual regression demonstrates virtually no reduction relative to the sigma of the "original" regression. Therefore, it can be concluded that $S_a(T_{FM})$ is sufficient with respect to the attenuation epsilon.

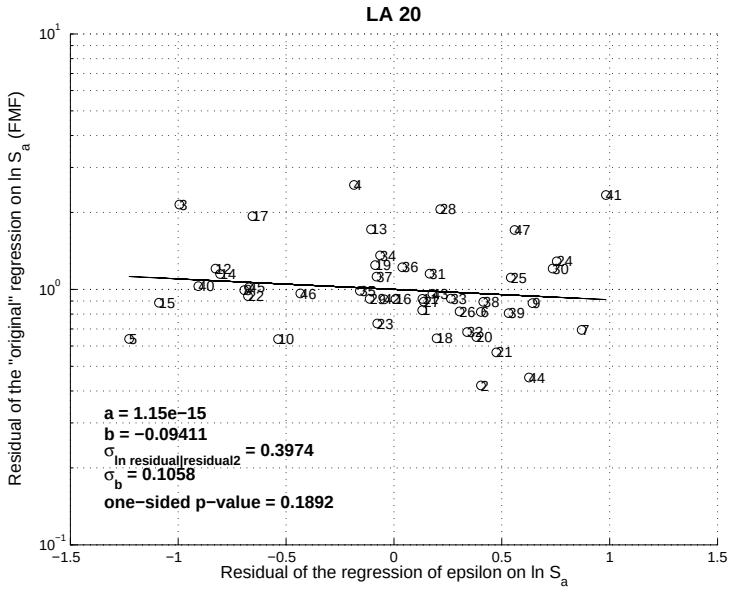

Figure 6-4 - Residual-residual plot for the epsilon of the attenuation law, ε, as a second independent variable for predicting the structural response for LA 20 structure, combined record selection.

6.9.2 System with short period: Generic SDOF structure

The example case of a structure with long fundamental period was discussed in the previous section. It was observed that the FMF spectral acceleration is sufficient with respect to each of the ground motion characteristics, magnitude M, rupture distance R_{rup}, and the attenuation epsilon, ε.

It is also of interest to investigate the sufficiency of $S_a(T_{FM})$ for a system with short period. This is because the non-linear displacement response of a high-frequency SDOF system is expected to show dependence on frequencies lower than the FMF frequency, which can be due to the period-elongation phenomenon (see Medina, 2002). The dependence of the response on periods longer than that of FMF's, may demonstrate itself in terms of the dependence on spectral shape factor. This dependence may be more pronounced in the high-frequency period range because of the steep slope of the acceleration spectrum in this region.

As the second example case, a short-period (T=0.1) SDOF system is modeled having bilinear hysteretic behavior with a strain hardening ratio equal to $\alpha = 0.03$ and a yield strength equal to $M_P = 5000\,k-in$. By definition, the displacement response of such an SDOF system is

proportional to the spectral acceleration in the linear-elastic range, meaning that the maximum displacement response shows zero record-to-record variability for a given $S_a(T_{FM})$. However, the displacement response in the non-linear range is not strictly proportional to the spectral acceleration and demonstrates record-to-record variability for a given spectral acceleration level. Hence, it is important to adjust the yield strength of this SDOF system in order to ensure that the dynamic displacement response for this study is in the non-linear range. Studying possible dependencies of response on ground motion characteristics decides whether they can (further) explain the record-record variability in the data due to nonlinear behavior.

Figure 6-5 illustrates the static pushover curve for the bi-linear SDOF model structure. It can be observed that the onset of inelastic behavior takes place at a drift angle equal to 0.0005. This is going to be helpful in evaluating the ductility range for the dynamic non-linear response of this SDOF system later in this section.

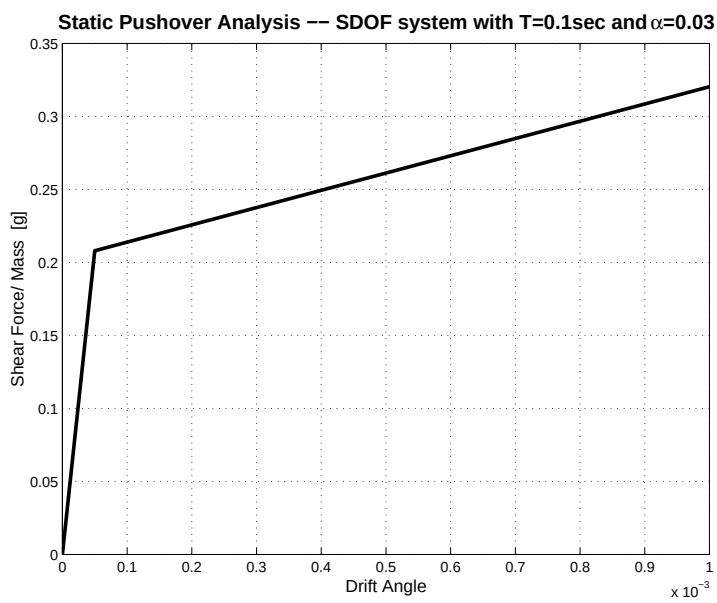

Figure 6-5 - The static pushover curve for a bi-linear SDOF system with T=0.1sec, $\xi = 0.05$, (strain hardening ratio) $\alpha = 0.03$, and $M_P = 5000\,k-in$

In Figure 6-6, the maximum dynamic displacement response, $\theta_{\max}$, of the SDOF model structure with period, T=0.1, and damping ratio, $\xi = 0.05$, to the combined record selection, is plotted versus $S_a(T_{FM})$. The straight line in the figure illustrates the result of the linear regression of $\ln\theta_{\max}$ on $\ln S_a(T_{FM})$ in the logarithmic scale, also referred to as the "original" regression. The RMS of regression residuals or the sigma of the original regression, $\sigma_{\ln\theta_{\max}|S_a}$, is reported as 0.83

on the figure. Compared to the sigma of the original regression for the LA 20, the sigma of the original regression for the SDOF system is about two times larger. It should also be noted that the linear regression slope parameter (the *b-value* reported on the figure) is equal to 1.6, which is much larger than the slope parameter reported for the LA20 (b=0.65). This b value implies the "softening" that is anticipated to cause this system to be sensitive to ground motion frequency content at frequencies less than its natural frequency. The maximum displacement response values in the figure range between 0.0001 and 0.01, which corresponds to a ductility range of 1 to 20. The large ductility ratios indicate that the displacement response is in the non-linear range. The large record-to-record variability in the response, indicated by the relatively large sigma value, is also typical of an SDOF system with a short elastic period in the non-linear range (Medina, 2002, Miranda, 2001, and Shome 1999).

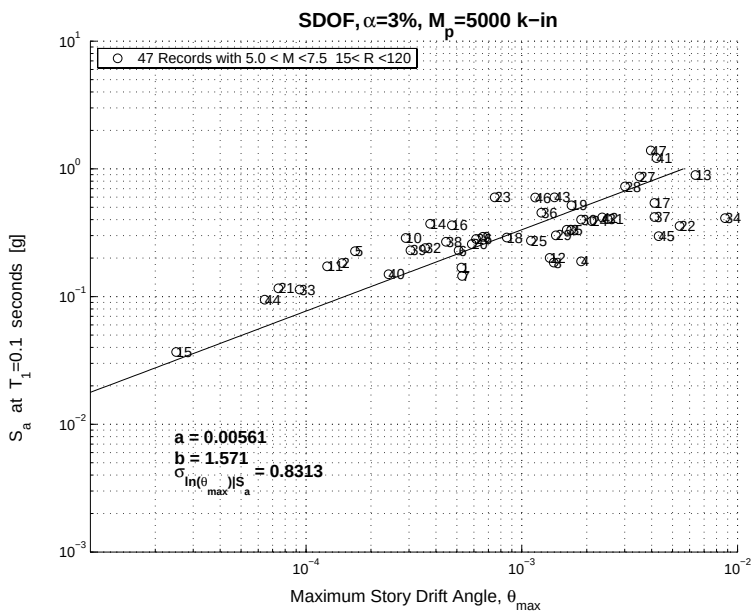

Figure 6-6 - The dynamic displacement response of the bi-linear SDOF model structure with T=0.1, damping $\xi = 5\%$, and $Mp = 5000\,k-in$ to the combined record selection

The sufficiency of $S_a(T_{FM})$ with respect to the magnitude in investigated in Figure 6-7. Figure 6-7 is a residual-residual plot for magnitude as a second regression variable. A slight negative trend between the response residuals and the residuals of the regression of magnitude on S_a is observed. However, the p-value is too large for the trend to be significant.

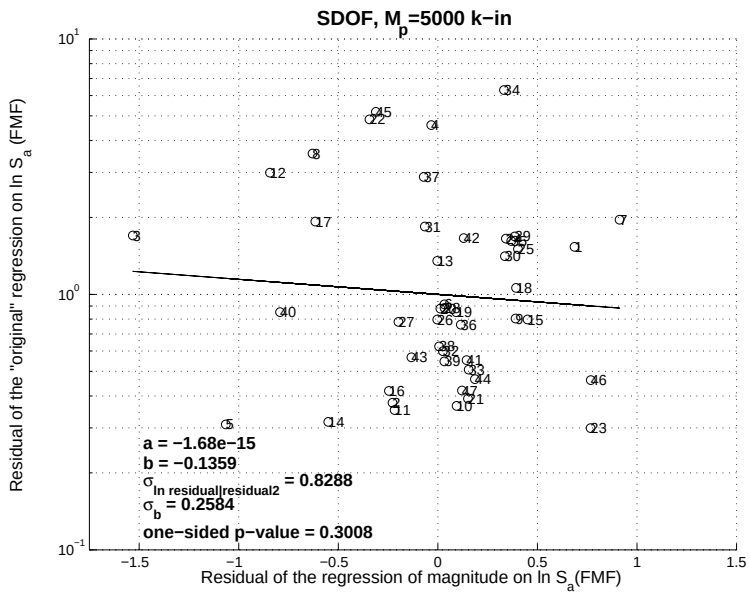

Figure 6-7 - Residual-residual plot for magnitude as a second independent variable for predicting the response of an SDOF system, combined record selection

Also, the sigma of the residual-residual regression (reported on the figure) is equal to $\sigma_{\ln residual|residual2} \approx 0.83$, which is equal to the sigma of the original regression ($\sigma_{\ln \theta_{\max}|S_a} = 0.83$). This implies that the addition of magnitude as a second regression variable does not decrease the dispersion of the response with respect to the regression prediction. Thus, it can be concluded that $S_a(T_{FM})$ is sufficient with respect to magnitude even for this very short-period system of large ductilities.

Figure 6-8 is the residual-residual plot for the rupture distance, R_{rup}, as a second regression variable. It can be observed that the two ground motions with large rupture distances are mainly responsible for the negative trend (judged by the seemingly large absolute value of the slope). However, the large variability of response residuals around the regression line causes the p-value to be very large. Hence, the observed slope is not in fact significantly different from zero. Also, the rupture distance, R_{rup}, does not reduce the dispersion of response with respect to regression prediction ($\sigma_{\ln residual|\ln residual2} = 0.82$), as a second regression variable. Hence, $S_a(T_{FM})$ is also sufficient with respect to the rupture distance, R_{rup}.

Figure 6-9 is the residual-residual plot for the normalized residual (epsilon) of the attenuation law, ε, as a second regression variable. Judging from the *p-value* for the slope, it can be observed that there is no significant trend between the two sets of residuals.

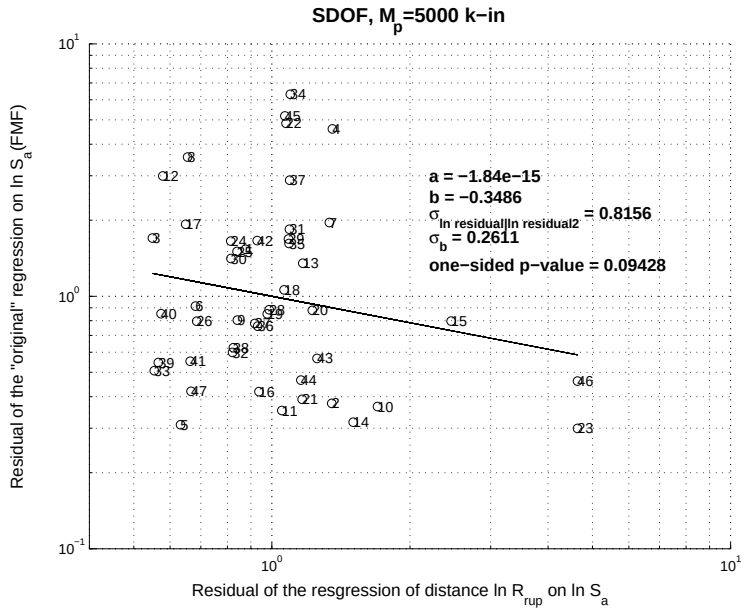

Figure 6-8 - Residual-residual plot for distance as a second independent variable for predicting the maximum inter-story drift angle, SDOF system, combined selection.

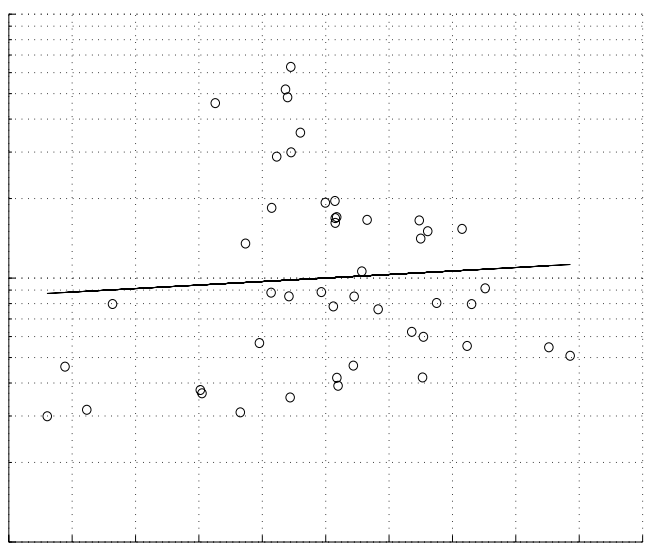

Figure 6-9 - Residual-residual plot for the normalized residual of the attenuation law, ε, as a second independent variable for predicting the structural response for SDOF system, combined record selection.

This observation is confirmed by the reported sigma of the residual-residual regression ($\sigma_{\ln residual|\ln residual2} \approx 0.83$), which is equal to the sigma of the "original" regression (reported on Figure 6-6). Hence, S_a is also sufficient with respect to the normalized residual (epsilon) of the attenuation relation, ε.

6.10 Studying the dependence of the displacement-based response given $S_a(T_{FM})$ on the spectral shape factor at period T, $R(T, T_{FM})$

In the previous section, the sufficiency of $S_a(T_{FM})$ with respect to ground motion characteristics, M, R_{rup}, and, ε, was established for two example cases with short and large FMF's. As was discussed, this also implies that none of the ground motion characteristics studied above, as a second regression variable, is going to (further) reduce the variability of the response around linear regression prediction.

In this section, the dependence of the displacement-based response, once it is conditioned on the FMF spectral acceleration, on the shape of the elastic acceleration spectrum is discussed. The spectral shape factor at period T, $R(T, T_{FM})$ is the variable that reflects the effect of the spectral shape. Recall that if this dependence is confirmed, and if the shape factor is also found to depend on magnitude, it would be expected that $S_a(T_{FM})$ would not be sufficient with respect to magnitude, contrary to what was found in the previous section. Further, it can be argued that establishing the dependence of the response given $S_a(T_{FM})$ on the spectral shape factor is equivalent to stating that the pair of $S_a(T_{FM})$ and $R(T, T_{FMF})$ as a vector-valued intensity measure is more "efficient" than $S_a(T_{FM})$ only. In other words, the vector *IM*, $\{S_a(T_{FM})$, $R(T, T_{FM})\}$, has $S_a(T_{FM})$ representing spectral "amplitude" at FMF as its first element, and $R(T, T_{FM})$ representing spectral "shape" at period T as the second element.

The procedure followed in this section for establishing the dependence of the displacement-based response (given $S_a(T_{FM})$), on $R(T, T_{FM})$ is similar to the one followed in order to investigate the sufficiency of $S_a(T_{FM})$ in the previous sections. In the same manner, the spectral shape factor $R(T, T_{FM})$ is regarded as a second regression variable, and the residual-residual plots are used to study the effect of shape factor in reducing the dispersion. It is important to note that this section

only presents a brief discussion of the role of spectral shape factor in increasing the efficiency in response predictions, and does not delve into the complexities and limitations of implementing a vector-based intensity measure. In summary, the main argument in this section is to relate the shape-dependence of the response to possible dependence on magnitude and hence explain why magnitude is generally believed to affect the response more than the other ground motion characteristics.

Similar to the previous section, the discussion here is divided into two parts, with each part focusing on one of the two example cases presented before.

6.10.1 System with large first-mode period: LA 20 story Results

The effect of spectral shape factor as a second regression variable is studied here for the LA 20 model structure. In the following, the residual-residual plot for spectral shape factor at its second mode frequency (*SMF*) with T_2=1.3 is presented and discussed in detail. The discussion is followed by studying the effect of the spectral shape factor at a period, T, as the second regression variable, from the point of view of the reduction in the dispersion around the regression prediction. This leads to finding an optimal period at which the dispersion is minimum, or in other words the pair $\{ S_a(T_{FM}) , R(T, T_{FM}) \}$ has maximum efficiency.

Since LA 20 is not a first-mode dominated structure, the spectral shape factor $R(T_{SF}, T_{FM})$ is a potentially important variable to consider as the second regression variable. The residual-residual plot for $R(T_{SF}, T_{FM})$ as a second regression variable is plotted in Figure 6-10.

Unlike the residual-residual plots in section 6.9, the residuals in Figure 6-10 demonstrate a clear and positive trend. The p-value is zero, which confirms that the slope of the line is significantly different from zero. Also the reported sigma of the residual-residual regression, 0.25, is significantly smaller than the sigma of the original regression, 0.40. This confirms the speculation that spectral shapes or spectral ordinates at higher frequencies might be effective in predicting the response for this tall building. Also, the significant reduction in the sigma of the regression indicates that the vector $\{ S_a(T_{FM}) , R(T_{SM}, T_{FM}) \}$ is going to be (relatively) more efficient in predicting the dynamic displacement response compared to the scalar $S_a(T_{FM})$ (also see, Vamvatsikos, 2002, and Shome 1999).

It is desirable to find the optimal period for the spectral shape factor as the second regression variable. The plot in Figure 6-11, illustrates the values for the sigma (dispersion measure) in the residual-residual regressions performed for a range of periods. For simplicity, the dispersions are normalized with respect to the sigma of the regression on S_a only. It can be observed that choosing the spectral shape for T=1.1 seconds (close to the second mode period) leads to more than 40% reduction in the dispersion compared to regression on S_a only. The periods corresponding to the first and second modes are marked on the figure. Also, the point marked by PGA represents the T=0 data point.

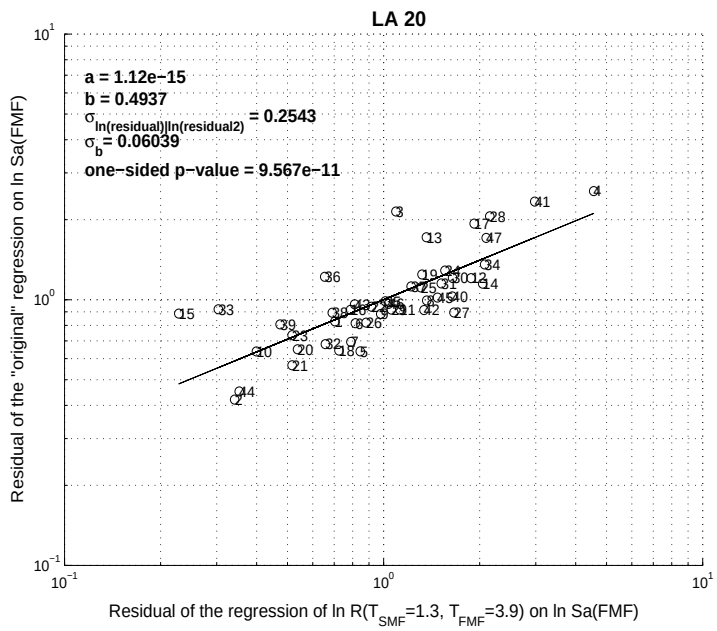

Figure 6-10 - residual-residual plot for spectral shape factor at SMF, as a second independent variable for predicting the structural response for LA 20 structure, combined record selection.

Generally-speaking, it can be observed that the (relative) dispersions decrease for the spectral shapes corresponding to the short-period range. This confirms the a priori speculations about the dependence of response on the higher mode spectral shapes. It should also be noted that the drift response of the LA 20 structure is generally smaller than 1%, indicating more-or-less elastic behavior. Hence, the dependence of the response (given FMF spectral acceleration) on the spectral shape at short periods seems to be consistent, as the effect of the higher modes on the response is more pronounced in the linear range of response. Later in this chapter (Section 6.14), the effect of the higher mode spectral shapes are going to be observed for the case where the response is in the non-linear range.

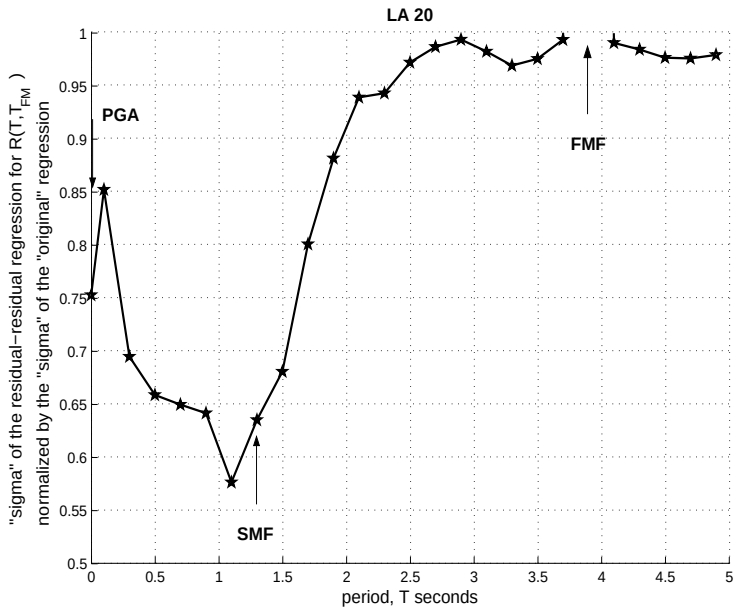

Figure 6-11 - The reduction in the "sigma" of the regression when the spectral shape factor at period T is used as a second independent variable in the regression, LA 20 structure, combined record selection.

6.10.2 SDOF systems with short period

It was observed in the previous section that for the 20-story MDOF structure, the spectral shape factor at frequencies higher than the FMF could explain part of the variability observed in the residuals of the original regression on spectral acceleration. In this section, the dependence of the non-linear response of the bi-linear SDOF system, visited earlier in this chapter, on the shape of the spectrum is studied. Although in the case of an SDOF system higher modes do not exist, it is expected that for the higher ductilities the system behaves as if it has an elongated effective period. Thus, the spectral shapes for periods longer than T=0.1, may play a significant role in explaining the variability observed in the response of the SDOF system.

In order to investigate the dependency of response of the SDOF system on the spectral shapes for periods longer than T=0.1, the residuals of response against the residuals of the spectral shape for T=0.3 are plotted in Figure 6-12. Judging from both the p-value and the reported sigma value, a significant positive trend in the plot can be observed. The p-value is infinitesimal, which indicates that the slope of the regression line is significantly different from zero; and the sigma is reduced by 35% compared to the sigma of the original regression in Figure 6-6. This confirms the speculations about the significance of the spectral shapes for periods longer than the first-mode

period in explaining the variability observed in the nonlinear response of the SDOF system with a very short period.

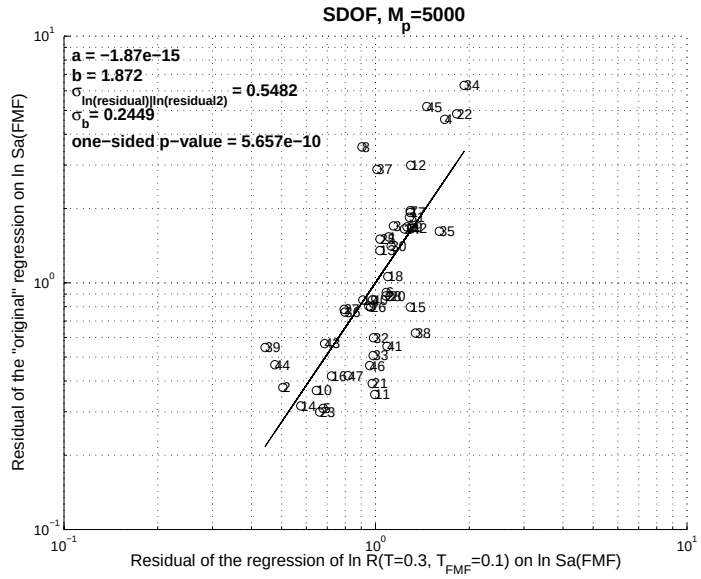

Figure 6-12 - The residual-residual plot for the shape factor at T=0.3 as a second independent variable for predicting the structural response for SDOF system with T=0.1, "combined" record set

The same steps explained above (for the spectral shape factor at T=0.3), are repeated over a range periods and the resulting relative dispersions are plotted versus period in Figure 6-13. Similar to the previous section, the sigma values (the sigma of the residual-residual regression) for each period are normalized with respect to the sigma of the original regression on spectral acceleration at T=0.1. It can be observed that the spectral shape factors for periods between 0.5 and 1 second lead to reductions up to 40% in the dispersion. This is consistent with the earlier observations for the spectral shape at T=0.3. In summary, the displacement-based response of this high-frequency bi-linear SDOF system is strongly dependent on spectral shapes at periods longer than that of the FMF. This observation is consistent with the elongation of the effective period in the high-ductility range.

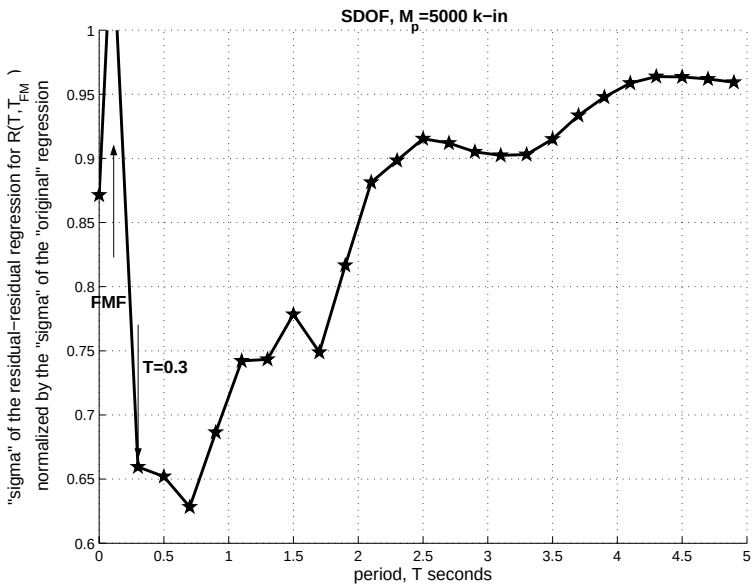

Figure 6-13 - The normalized sigma of the residual-residual plot for the spectral shape factor at period T with respect to the sigma of the original regression on spectral acceleration at T=0.1.

6.11 Discussion: The correlation between spectral-shape factor and magnitude

It was observed in the previous sections that for a given value of $S_a(T_{FM})$, the displacement-based response of the two example structures demonstrate statistically significant dependence on the spectral shape factor. The dependence on the spectral shape factor may be observed for structures with a wide range of first-mode periods. For example, a first-mode dominated structure might undergo considerable damage when subjected to a ground motion excitation. This will cause the structure to behave as a softer system with a longer effective period; hence, the spectral shape for a longer period might be effective as a second regression variable. For a tall structure with long first-mode period, the displacement-based response is most likely to be dictated by higher modes. In this case the spectral shapes for periods shorter than that of the FMF may be more effective as second regression variables.

On the other hand, since they are physically limited in the production of longer period waves, smaller magnitude records are expected to have comparatively stronger short-period (high-frequency) energy content. Thus, one would expect to observe a negative correlation between the spectral shape factor for second-mode period and the magnitude. This hypothesis is tested for the suite of records used in this chapter. The spectral shape factors for the suite of records at a period equal to T=1.3 seconds (corresponding to second mode frequency for the 20-story building), normalized to the FMF spectral acceleration at a period to T= 3.9 seconds are plotted versus

magnitude in Figure 6-14. The anticipated inverse trend can be observed from the data points and also the negative slope of the line fitted to the data. The slope of the fitted line indicates roughly a factor of 50% reduction in this particular shape-factor for a magnitude increase of one unit. The reported *p-value* for the slope of the line in Figure 6-14 indicates that there is an "effectively" significant correlation between the spectral shape and magnitude.

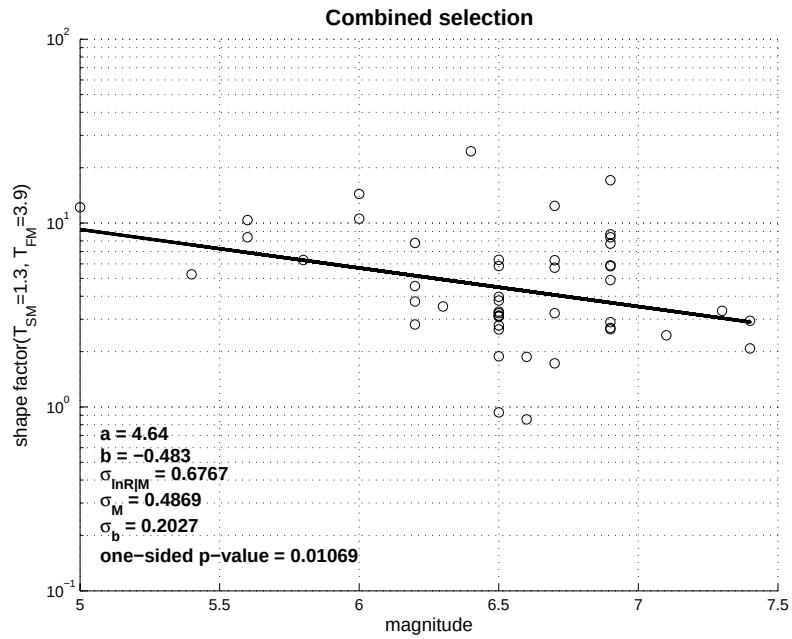

Figure 6-14 - Combined selection, shape factor for T=1.3 sec and T=3.9 sec plotted against moment magnitude

Alternatively, one can use the attenuation relation predictions for the spectral shape versus magnitude in order to test the hypothetical correlation between the spectral shape factor and magnitude. The attenuation relation prediction for the log of the spectral acceleration at period T can be calculated from Equation 6-1. The mean (of the log) spectral shape factor, $R(T_1, T_2)$, can be predicted by subtracting the mean (of the log) attenuation predictions for spectral accelerations at periods T_1 and T_2 respectively (Equation 6-2a):

$$E[\ln R(T_1, T_2)] = E[(\ln S_a(T_1) - \ln S_a(T_2))] = \Delta f(M, R_{rup}) \qquad (6\text{ - }2a)$$

$$\sigma^2{}_{\ln R(T_1,T_2)} = \sigma^2{}_{\ln S_a(T_1)} + \sigma^2{}_{\ln S_a(T_2)} - 2 \cdot \rho_{\ln S_a(T_1), \ln S_a(T_2)} \cdot \sigma_{\ln S_a(T_1)} \cdot \sigma_{\ln S_a(T_2)} \qquad (6\text{ - }2b)$$

Also the squared standard deviation (variance) for the shape factor can be calculated by combining the attenuation predictions for the standard deviation of the natural logarithm of

spectral acceleration at periods T_1 and T_2 (Equation 6-2b). It should be noted that expression for standard deviation in Equation (6-2b) includes the correlation coefficient between the (natural log of) the spectral acceleration values at periods T_1 and T_2. Figure 6-15 illustrates the results of attenuation predictions for the spectral shape factors at $T_1 = 1$ and $T_2 = 4$ (approximately the second-mode and the first-mode periods for the 20-story building).

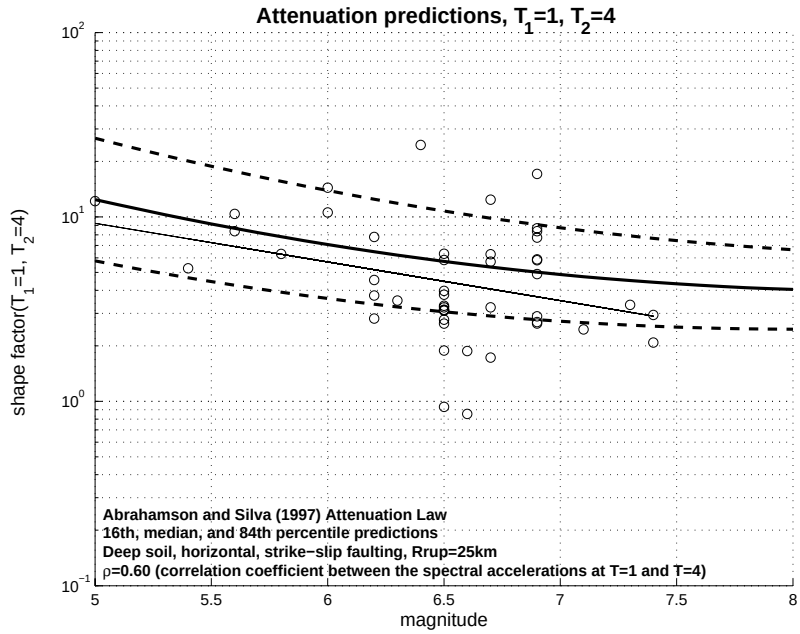

Figure 6-15 - Attenuation prediction for shape factor at T=1 sec ($\approx T_{SM}$) and T=4 sec ($\approx T_{FM}$) plotted against magnitude (thick lines). The thin is the linear regression prediction based on the "combined" ground motion record set.

The spectral shape factors are predicted using Abrahamson and Silva (1997) attenuation relations for the horizontal component of the ground motion. It has been assumed that the style of faulting is strike-slip and the site's soil type is deep soil. In order to calculate the standard deviation of the predicted shape factor from the Equation 6-2b, the correlation coefficient between the spectral acceleration values at the two periods under consideration should be estimated. For the two periods, 1 and 4, a 60% correlation between the (log of the) corresponding spectral acceleration values is assumed (based on the observed correlation for the ground motions used in this chapter). Figure 6-15 illustrates the 16th, median and 84th percentiles of the predicted shape factors against the shape factors calculated from the suite of records.

It can be observed that most of the spectral shape factors for the suite of records (the combined selection) fall between the 16% and 50% attenuation law predictions. The slope of the predicted median of the attenuation shape factor is roughly the same as the slope of the line fitted to the data points. This also confirms a "weak" correlation between the spectral shape factor and ground motion magnitude for $T_1 = 1$ and $T_2 = 4$. It is also interesting to study the dependence of the spectral shape factor at very short periods on ground motion magnitude. The conclusion may be useful in understanding the dependence of the response of the high-frequency SDOF system on magnitude.

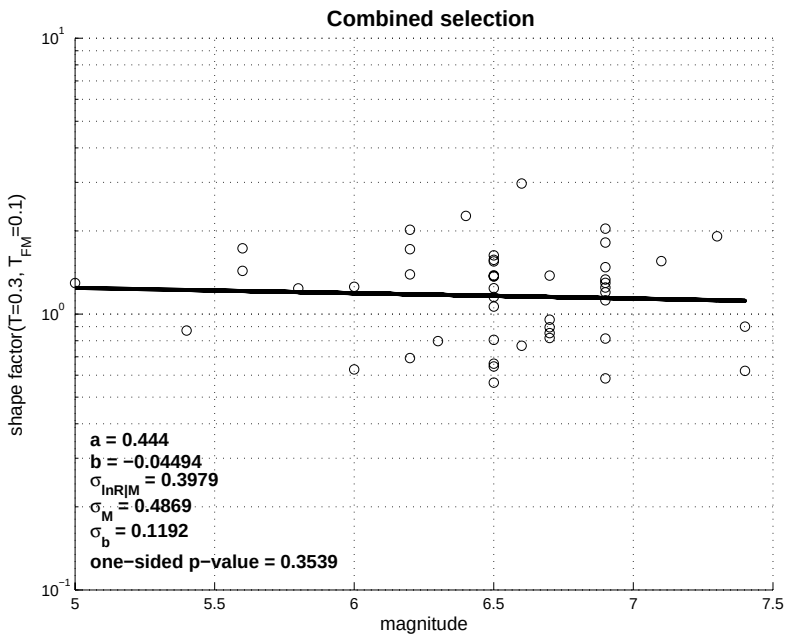

Figure 6-16 - Combined selection, shape factor for T=0.3 sec and T=0.1 sec plotted against moment magnitude

Therefore, the spectral shape factors at periods $T_1 = 0.1$ and $T_2 = 0.3$ are plotted in Figure 6-16 for the suite of records used in this chapter. It can be observed that there is no particular trend in the data; this is also confirmed by the close-to-zero slope of the line fitted to the data and the large *p-value* for the slope. Nonetheless, the attenuation relation prediction for the shape factor at $T_1 = 0.1$ and $T_2 = 0.3$ in Figure 6-17 indicates a slightly positive trend with regard to magnitude. Nevertheless, since the two periods, T_1 and T_2 are both in the high-frequency range, the ratio between their corresponding spectral acceleration values may not be strongly dependent on magnitude.

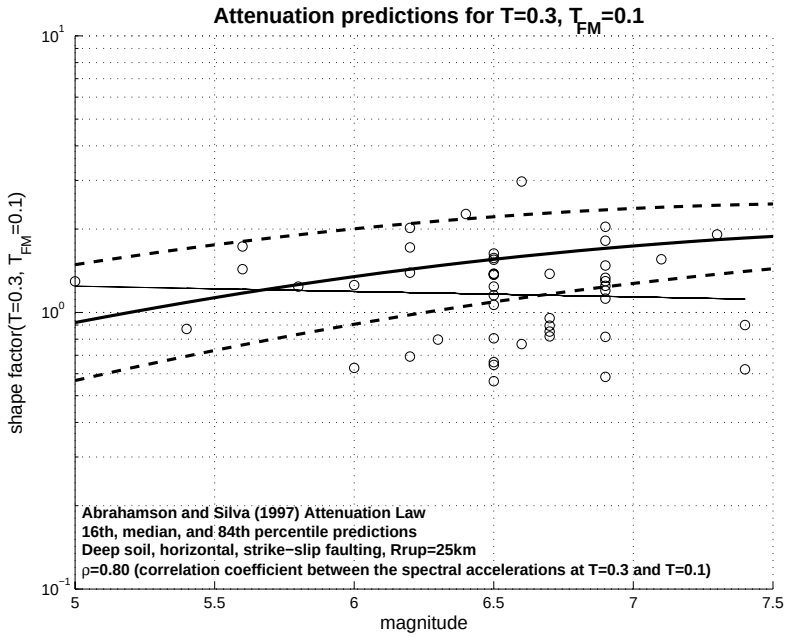

Figure 6-17 - Combined selection, shape factor for T_{FM}=0.1 sec and T=0.3 sec plotted against magnitude

6.12 Discussion: Does magnitude matter?

The ground motion magnitude is probably the most likely ground motion characteristic variable to affect the structural response. This section is going to discuss the effect of magnitude on the structural response from the point of view of its relation to the shape of the acceleration spectrum.

It was established in Section 6.10 that, given the FMF spectral acceleration, the structural response is positively correlated to spectral shape factor at a period different than FMF. For the case of the 20-story structure, the response is most strongly correlated to spectral shape factors at periods shorter than FMF and close to the second-mode frequency (SMF). For the high-frequency SDOF system, the response is most strongly correlated to shape factors at periods longer than FMF. Consistent with the above observations, the relation between shape factor and magnitude was investigated for the spectral shape factors at T=1.3 (SMF period for 20-story structure) and T=0.3 (3 times the FMF period for the SDOF system). For the 20 story building, the spectral shape factor at SMF period was negatively correlated to magnitude with a relatively large dispersion around the line fitted to the data. However, for the high-frequency SDOF system no significant correlation was observed between the shape factor at T=1.3.

The dependence of response on the shape factor and also the negative correlation between the shape factor and magnitude in the case of a long-period structure like the 20-story structure may suggest that the response is in turn (negatively) related to magnitude. However, this prediction seems to be contradicted by the results drawn from the residual-residual plot for magnitude in Figure 6-3. These results indicate that given the FMF spectral acceleration, the displacement-based response for the 20-story structure is not significantly dependent on magnitude. A closer look at Figure 6-3 reveals that given the FMF spectral acceleration the response is indeed negatively correlated with magnitude, but the slope of the residual-residual regression line is very small and its corresponding *p-value* is quite high. Nevertheless, this may be explained by the (relatively large) dispersion around the line fitted to the shape factor-magnitude data points in Figure 6-14 and the (non-infinitesimal) *p-value* for the slope of this line. In summary it can be argued that, although the response may suggest some minor dependence on magnitude for the 20-story structure, the large variability in the data-points causes the observed dependence not to be (statistically) significant. Further, regression analyses that show dependence of response (given FMF spectral acceleration) on shape factor and also shape factor on magnitude, do not necessarily imply that there must be a positive (linear) correlation between response (given FMF spectral acceleration) and magnitude. Hence, it can be concluded that despite the reasonable expectations that (given FMF spectral acceleration) magnitude might provide some additional predictive power, there is no evidence to this effect in the data for either the very long or very short period systems studied here. This conclusion is consistent with the conclusions others have reached for moderate-period, first-mode dominated structures (e.g., Bazzurro 1994, Shome 1999, Luco, 2002).

6.13 Observations for the SDOF system with a different yield strength

In the previous sections, the sufficiency of $S_a(T_{FM})$ with respect to ground motion characteristics such as magnitude, distance and "epsilon" of the attenuation law, was established for a short-period SDOF system. It was also observed that given the FMF spectral acceleration, the displacement-based response of such SDOF system demonstrates a strong dependence on spectral shape factors at longer periods (due to the elongation of effective period for high-ductility range). It is important to investigate whether these observations will still hold for a different degree of non-linearity in the system. Thus the displacement-based response of the bi-linear SDOF system is studied for different ductility levels by changing the yield strength of the system. In Section

6.9.2, the dynamic displacement response of an SDOF system with a yield strength equal to $M_P = 5000\,k-in$ was studied. According to the range of ductility observed in the response (Figures 6-5 and 6-6), the system is already in a highly non-linear range. In this section, the yield strength is scaled up to $M_P = 15000$ and $M_P = 10000$ in order to achieve lower ductility levels in the displacement response. In Figure 6-18, the response of the SDOF system with $M_P = 15000$ (three times the original strength) to the "combined" set of records is plotted. It is apparent that response is in a lower ductility region since the yield drift angle shown in the static pushover curve for $M_P = 5000\,k-in$ in Figure 6-5 is also going to be scaled up; and also the displacement-based response in Figure 6-18 is generally smaller than those of Figure 6-6. In contrast to the similar plot in Figure 6-6 corresponding to the yield strength of $M_P = 5000\,k-in$, an more-or-less linear portion can be observed in the displacement-based response in Figure 6-18

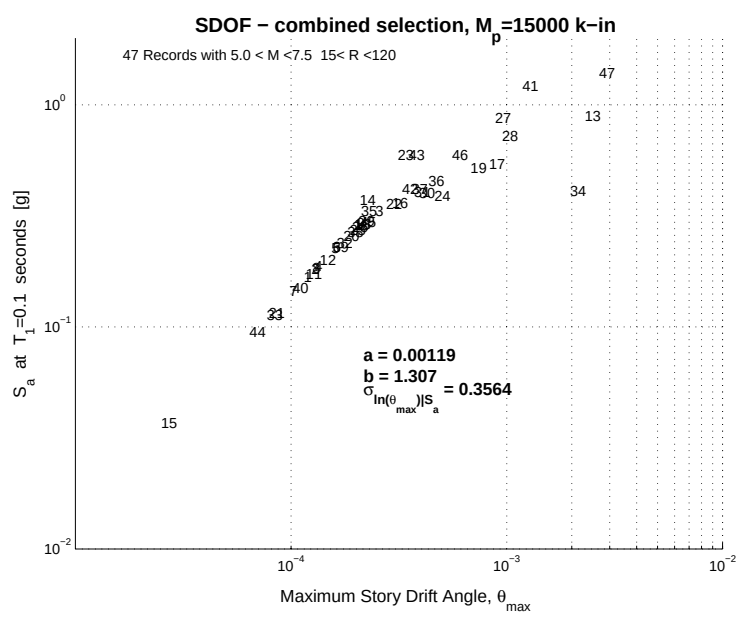

Figure 6-18 - The SDOF system with $M_P = 15000$ subjected to the combined record selection

The same steps described in Sections 6.9.2 and 6.10.2 are followed here in order to investigate the sufficiency of $S_a(T_{FM})$ with respect to ground motion characteristics and also to investigate the dependence of response on spectral shape factors at periods larger than T=0.1, when the yield strength is scaled up by factor of 2 and 3. The results are tabulated for brevity. Table 6-2 lists the parameters of the regression of response on the spectral acceleration. It can be observed that the dispersion increases with decreasing yield strength. This is expected as the dispersion increases for displacement response in higher ductilities. Also for higher yield strength levels a larger

number of response data points are still behaving elastically, which for an SDOF systems implies zero dispersion locally. The same trend is observed for the *b* value (the slope parameter in the log-log scale) that is increasing with decreasing strength. This is also consistent, as a larger b value is associated with "softening" behavior in a non-linear system.

Regression on S_a	a	b	$\sigma_{\ln \theta_{max} \mid S_a}$
M_p=5000 k-in	0.0056	1.571	0.8313
M_p=10000 k-in	0.0023	1.562	0.6091
M_p=15000 k-in	0.0012	1.307	0.3564

Table 6-2 - The results of the regression of response on S_a for different yield strengths

Tables 6-3 and 6-4 outline the parameters reflecting the importance of ground motion characteristics, M, R_{rup}, and ε, and spectral shape factors for T=0.3 and T=0.5, as a second regression variable in addition to $S_a(T_{FM})$ (for two different yield strength values). The same as Section 6.9.2, the sufficiency of $S_a(T_{FM})$ with respect to the three ground motion characteristics, M, R_{rup}, and ε, is established for higher yield strength values (10000 k-in and 15000 k-in). This is observed through significant *p-values* as well as negligible reduction in dispersion for both strength levels. This confirms the sufficiency of $S_a(T_{FM})$ for different strength levels and hence different ductility levels. The dependence of the displacement-based response on spectral shapes at longer periods can also be observed from Tables 6-3 and 6-4 for both strength levels. Although such dependence is more pronounced (i.e., smaller *p-values,* more reduction in the dispersion, and steeper slopes) for the case with smaller strength ($M_P = 10000$). This can be explained by the fact that for the case with smaller strength, the response lies in a larger ductility range, which implies more drastic elongation of the effective period.

It should also be noted that for the largest strength level, when the ductitilies are the mildest, there is little benefit to the shape factor. This could be expected since in the linear range there is no benefit in adding the spectral information at other periods, as the spectral acceleration is the perfect predictor.

M=10000 k-in	b	$\frac{\sigma_{residual\ |residual\ 2}}{\sigma_{\ln\theta_{\max}\ |\ln S_a}}$	p-value
M	-0.013	1	0.472
Rrup	-0.03	1	0.484
ε	0.013	1	0.455
R(T=0.3, T_{FMF}=0.1)	1.065	0.81	0
R(T=0.5, T_{FMF}=0.1)	0.693	0.78	0

Table 6-3 - The importance of ground motion characteristics, M, R_{rup}, and ε, and two different spectral shape factors as the second regression variable, SDOF system $M_P = 10000$ (moderate ductilities)

M=15000 k-in	b	$\frac{\sigma_{residual\ |residual\ 2}}{\sigma_{\ln\theta_{\max}\ |\ln S_a}}$	p-value
M	0.057	0.997	0.3
Rrup	-0.09	0.993	0.48
ε	0.019	0.999	0.39
R(T=0.3,T_{FMF}=0.1)	0.343	0.947	0.013
R(T=0.5,T_{FMF}=0.1)	0.267	0.91	0.002

Table 6-4 - The importance of ground motion characteristics, M, R_{rup}, and ε, and two different spectral shape factors as the second regression variable, SDOF system $M_P = 15000$ (low ductilities)

6.14 Observations for LA 20 story building when the ground motion records are scaled

It has been established in Section 6.9.1 that for a long-period 20-story structure, $S_a(T_{FM})$ is sufficient with respect to the ground motion characteristics, and that given $S_a(T_{FM})$ the displacement-based response is dependent on spectral shape factors at periods shorter than FMF period. In this section, the validity of such conclusions are investigated for the displacement-base response of the 20-story structure in a different ductility range.

In order to study the dynamic response of the 20-story building at a different ductility level, the ground motion records have been scaled by a factor of 3 so that the structure is "pushed" further into the non-linear regime.

In Figure 6-19, the displacement-based response of the LA 20 structure to the scaled ground motion records is plotted versus FMF spectral acceleration. It can be observed that the drift angles are larger than those in Figure 6-1 in Section 6.9.1 for the un-scaled records. The median drift is equal to 0.017 whereas in Figure 6-1 the median drift is equal to 0.0051. Also in ductility terms, the response to the scaled records is on average in a ductility range of 2 compared to the response in the un-scaled case where the response is effectively in the elastic range. The ductilities are calculated based on a yield drift angle of 1% obtained from static pushover results for the LA 20 building. (courtesy of Vamvatsikos, 2002).

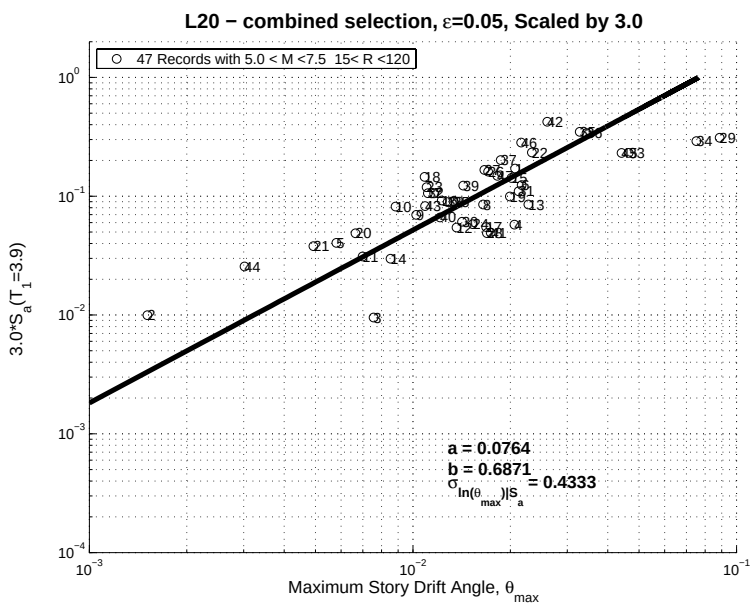

Figure 6-19 - Maximum inter-story drift angles for LA20 structure, combined selection scaled by a factor of 3

Table 6-5 lists the regression parameters for LA 20 building when subjected to the scaled ground motion records. It can observed that the intercept is larger compared to the one for the un-scaled response in Section 6.9.1 (Figure 6-1). The dispersion and the b value (log-log slope parameter) are also slightly larger in this case.

Regression on S_a	a	b	$\sigma_{\ln \theta_{\max} \mid S_a}$
scaled by 3	0.0764	0.6871	0.433
not scaled	0.0507	0.6553	0.401

Table 6-5 – The results of the regression of response on $S_a(T_{FM})$ for the case where the ground motion accelerations are scaled by a factor 3, LA 20 story building

Table 6-6 outlines the parameters reflecting the significance of M, R_{rup}, and ε, and second-mode shape factor as second regression variables in addition to the FMF spectral acceleration. This case of sufficiency with respect to magnitude is not as clear-cut as for the un-scaled records, however, Figure 6-20 illustrates the residual-residual plot for magnitude as a second variable. Visually, there is a mild trend but a single (magnitude 5) data point (number 3) is largely responsible for the appearance and for the marginally low *p-value* (0.068). (If this point is removed the p-value increases to 0.211). It can be observed that magnitude provides only a 2% reduction in standard deviation (0.42 versus 0.43). Finally, even if estimate of *b* is accepted as statistically significant (i.e., different from zero), its value (0.22) implies that the strength of dependence of response on magnitude is not great in practical terms. The value implies that change in magnitude of ± one-half magnitude unit implies only a ± 10% change in predicted response. Taken together with the clear lack of significance at lower ductility levels (when one would a priori expect a stronger dependence on magnitude), the conclusion that magnitude plays a minor, if any, role cannot be avoided.

scale factor= 3	b	$\frac{\sigma_{residual \mid residual\ 2}}{\sigma_{\ln \theta_{\max} \mid \ln S_a}}$	p-value
M	-0.2237	0.976	0.068
Rrup	-0.299	0.948	0.455
ε	-0.15	0.98	0.0866
$R(T_{SMF}=1.3, T_{FMF}=3.9)$	0.3886	0.826	0

Table 6-6 - The importance of ground motion characteristics and spectral shape factor as the second regression variable, LA 20 building $S.F. = 3.0$

It can also be observed from Table 6-6 that given the FMF spectral acceleration, the displacement-based response is positively correlated with the SMF spectral shape (at T=1.3). This

is due to the zero *p-value* and also due to significant reduction in dispersion (17%). However, the reduction in dispersion is smaller (by about half). As compared to the un-scaled case (when it was more than 35% in that case).

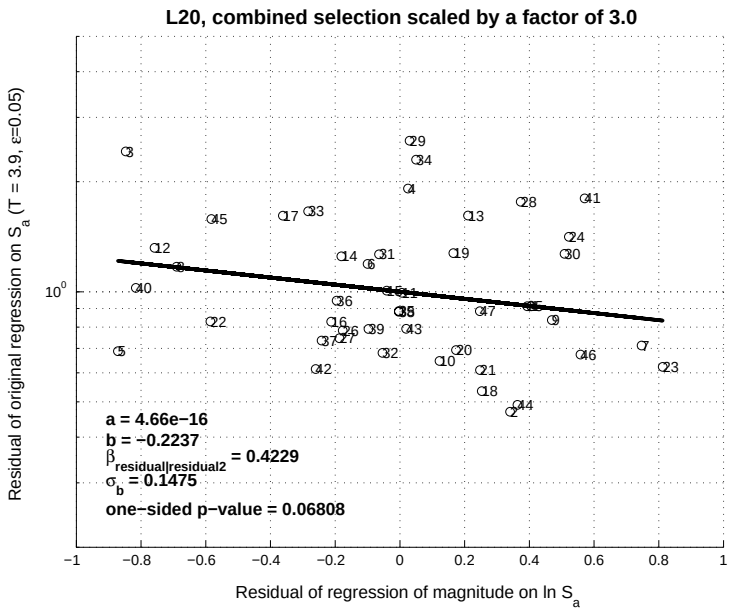

Figure 6-20- The residual-residual plot for magnitude as a second regression variable, the "combined" record set scaled by a factor of 3.

This may be explained by the stronger higher mode dependence for the response in the low ductility range. Figure 6-21 illustrates (square) RMS of the residual-residual regressions for the spectral shape factors at different periods normalized by the (square) RMS of the "original" regression on FMF spectral acceleration for the 20-story structure subjected to the "combined" set of records scaled by a factor of 3. It can be observed the maximum reductions in (square) RMS occur at period shorter or around the SMF period.

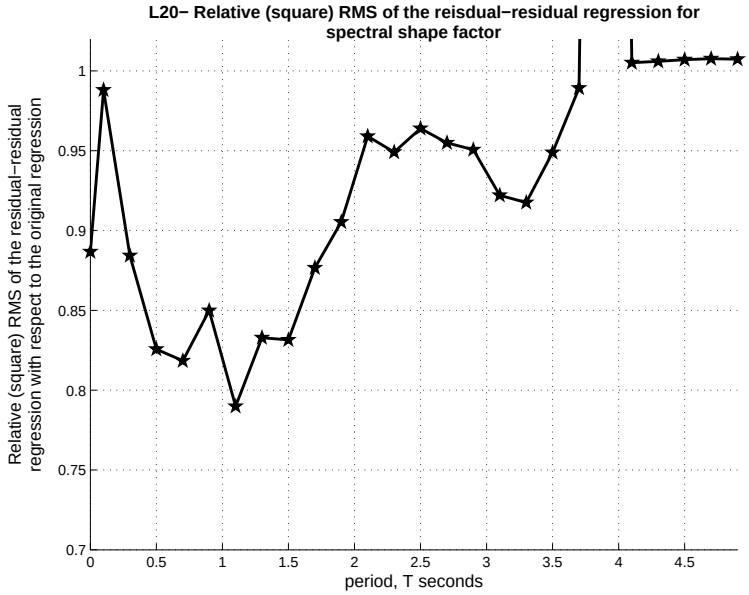

Figure 6-21 - Comparing the (square) RMS of the residual-residual regression for the shape factor at different periods with the (square) RMS of the "original regression" on FMF spectral acceleration, LA 20 structure, the "combined" record set scaled by a factor of 3.

6.15 Sufficiency and ground motion record selection

It was demonstrated in the previous sections how to establish the sufficiency of $S_a(T_{FM})$ with respect to ground motion characteristics, magnitude *M*, (source-to-site) distance R_{rup}, and the epsilon, ε. This section is going to discuss how establishing the sufficiency criterion is going to affect ground motion record selection.

To address this problem, it can be recalled first that the sample average and the sample variance of the relevant displacement-based response can be calculated as:

$$\bar{\theta}_{\max} = \hat{E}[\theta_{\max}] = \frac{1}{N_T}\sum_{i}^{N_T}\theta_{\max}^{(i)} \qquad (6-3)$$

$$s^2{}_{\theta_{\max}} = \hat{E}[\theta_{\max}{}^2] - (\bar{\theta}_{\max})^2 \qquad (6-4)$$

where $\hat{E}[.]$ denotes the expected value (mean) estimated by the sample average. The above equations can also be applied to the natural logarithm of the relevant displacement-based response for a given $S_a(T_{FM})$ or other intensity measure equals level, *x*:

$$\ln \eta_{\theta_{\max}|S_a(T)}(x) \cong \hat{E}[\ln \theta_{\max} \mid S_a(T)] = \frac{1}{N_T}\sum_{i}^{N_T} \ln \theta_{\max}^{(i)} \qquad (6 - 5)$$

$$\beta^2{}_{\theta_{\max}} \cong \sigma^2{}_{\ln \theta_{\max}} \cong \hat{E}[\ln \theta_{\max}{}^2 \mid S_a(T)] - (\hat{E}[\ln \theta_{\max} \mid S_a(T)])^2 \qquad (6 - 6)$$

Where the (log of) median has been approximated by the sample average of the logarithm of the response. However, for a lognormal variable the mean of the logarithm <u>is</u> equal to the logarithm of the median. Also, the squared standard deviation of the logarithm of response has been approximated by the sample variance of logarithm of the response. The next step is to expand the estimated median and the standard deviation (of the logarithm) can be "expanded" with respect to ground motion characteristics, *M*, R_{rup}, and ε:

$$\ln \hat{\eta}_{\theta_{\max|S_a(T)}}(x) = \sum_{i=1}^{N_M}\sum_{j=1}^{N_{R_{rup}}}\sum_{k=1}^{N_\varepsilon} \hat{E}[\ln \theta_{\max}(x, m_i, r_j, \varepsilon_k) \mid S_a, M, R_{rup}, \varepsilon] \;.\; p_{M,R_{rup},\varepsilon|S_a(T)}(m_i, r_j, \varepsilon_k \mid x)$$

(6 – 7)

where $\hat{\eta}(.)$ denotes the <u>estimated</u> median. For a selection of records consisting of N_T ground motion records the above expression can be expanded by dividing the chosen records into $N_M \times N_{R_{rup}} \times N_\varepsilon$ bins, in which each bin is represented by values, m_i, r_j, ε_k. $average(\ln \theta_{\max}(x, m_i, r_i, \varepsilon_i))$ is the estimated conditional mean (i.e., sample average) for the natural log of response in each bin, represented by values, m_i, r_j, ε_k, for a given spectral acceleration value, x and $p_{M,R_{rup},\varepsilon|S_a(T)}(m_i, r_j, \varepsilon_k \mid x)$ is the ratio of the number of ground motion the bin to the total number of ground motions, N_T, i.e., the fraction of records in bin (*i,j,k*).

In a similar manner, the conditional variance of the natural logarithm of response for a given spectral acceleration , *x*, can be expanded with respect to ground motion characteristics, *M*, R_{rup}, and ε:

$$\hat{\beta}^2_{\ln\theta_{\max}|S_a(T)}(x) = \sum_{i=1}^{N_M}\sum_{j=1}^{N_{R_{rup}}}\sum_{k=1}^{N_\varepsilon}\hat{E}[(\ln\theta_{\max}(x,m_i,r_j,\varepsilon_k))^2 \mid S_a(T),M,R_{rup},\varepsilon] \;.\; p_{M,R_{rup},\varepsilon|S_a(T)}(m_i,r_j,\varepsilon_k \mid x) - (\ln\hat{\eta}_{\theta_{\max}|S_a(T)}(x))^2 \quad (6-8)$$

Here, $\hat{E}[(\ln\theta_{\max}(x,m_i,r_j,\varepsilon_k))^2 \mid S_a(T),M,R_{rup},\varepsilon]$ denotes the expected value estimated by the conditional sample average of the squares of the natural logarithm (i.e., the estimated second moment) of structural response to ground motions in each bin represented by values m_i, r_j, ε_k, (for a given spectral acceleration value, *x*). In order to maintain the generality of the above equations, the spectral acceleration is presented by spectral acceleration, $S_a(T)$, evaluated at the period, *T*. Therefore, $S_a(T_{FM})$ is a special case of $S_a(T)$ evaluated at the period corresponding to FMF.

As it was stated in the beginning of this chapter, an intensity measure (e.g., $S_a(T_{FM})$) is sufficient if it renders the displacement-based response conditionally independent of the ground motion characteristics, for a given intensity level (e.g., $S_a(FM) = x$). The statistical equivalent to this statement is to establish that the conditional probability distribution for the displacement-based response of the structure for a given intensity level is independent of the ground motion characteristics, namely:

$$f_{\theta_{\max}|S_a(T)}(x) = f_{\theta_{\max}|S_a(T),M,R_{rup},\varepsilon}(x,m_i,r_j,\varepsilon_k) \qquad (6\text{ - }9)$$

for any m_i, r_j, ε_k value.

The sufficiency criterion can be also "approximated" in terms of the (conditional) statistical moments of the response being independent of the ground motion characteristics. For example, a "first-order measure" of the sufficiency criterion can be obtained by establishing that the first (conditional) moment of the response for a given spectral acceleration level, *x*, is independent of the ground motion characteristics:

$$E[\ln\theta_{\max}(x) \mid S_a(T)] = E[\ln\theta_{\max}(x,m_i,r_j,\varepsilon_k) \mid S_a(T),M,R_{rup},\varepsilon] \quad \text{for all } m_i, r_j \text{ and } \varepsilon_k \quad (6\text{ - }10)$$

For a lognormal random variable, the above equation can be written as the equality of the medians:

$$\hat{\eta}_{\theta_{\max}|S_a(T)}(x) \cong \hat{E}[\ln \theta_{\max} \mid (x, m_i, r_j, \varepsilon_k)] \qquad (6\text{-}11)$$

If a ground motion is sufficient with respect to the ground motion characteristics, it can be demonstrated that the two sides of Equation 6-7 will be always equal (by substituting $\hat{\eta}_{\theta_{\max}|S_a(T),M,R_{rup},\varepsilon}(x, m_i, r_i, \varepsilon_i)$ by $\hat{\eta}_{\theta_{\max}|S_a(T)}(x)$ in the equation):

$$\ln \hat{\eta}_{\theta_{\max}|S_a(T)}(x) \cong \sum_{i=1}^{N_M} \sum_{j=1}^{N_{R_{rup}}} \sum_{k=1}^{N_\varepsilon} \ln \hat{\eta}_{\theta_{\max}|S_a(T)}(x) \;\; . \;\; p_{M,R_{rup},\varepsilon|S_a(T)}(m_i, r_j, \varepsilon_k \mid x)$$

$$= \ln \hat{\eta}_{\theta_{\max}|S_a(T)}(x) \cdot \sum_{i=1}^{N_M} \sum_{j=1}^{N_{R_{rup}}} \sum_{k=1}^{N_\varepsilon} p_{M,R_{rup},\varepsilon|S_a(T)}(m_i, r_j, \varepsilon_k \mid x) = \ln \hat{\eta}_{\theta_{\max}|S_a(T)}(x)$$

The above conclusion is based on the fact that the sum of the fractions $p_{M,R_{rup},\varepsilon|S_a(T)}(m_i, r_i, \varepsilon_i \mid x)$ is equal to unity. A "second order measure" of sufficiency criterion in Equation 6-9 can be expressed in terms of the (conditional) second moment of the response:

$$\hat{E}[(\ln \theta_{\max}(x))^2 \mid S_a(T)] = \hat{E}[(\ln \theta_{\max}(x, m_i, r_j, \varepsilon_k))^2 \mid S_a(T), M, R_{rup}, \varepsilon] \quad \text{for all } m_i, r_j \text{ and } \varepsilon_k \qquad (6\text{-}12)$$

Similarly, it can be demonstrated that the two sides of Equation 6-8 will always be equal if the second order approximation to sufficiency is established.

It is demonstrated above that if the candidate intensity measure is sufficient with respect to ground motion characteristics, careful selection of ground motion records is not essential, as the displacement response for a given intensity level is independent of the ground motion characteristics. It was also discussed that a "first-order" approximation to the sufficiency criterion results in the (conditional) median of the displacement response for a given intensity level being independent of the ground motion characteristics. A "second-order" approximation to the sufficiency criterion results in the conditional fractional standard deviation (i.e., the standard deviation of the natural logarithm) of the displacement-based response the being independent of the ground motion characteristics.)

It was described how to establish sufficiency by using the residual-residual plots earlier in this chapter. Now, one might question how that method for establishing sufficiency relates to the discussions above. The residual-residual plots can reveal possible dependence of the response on a ground motion characteristic variable once they are both normalized with respect to the candidate intensity measure. It can be argued that this is approximately equivalent to establishing the "first-order" approximation to the sufficiency criterion stated above, because it is based on determining whether there is linear dependence of the (conditional) mean of the (log) of response on magnitude (for example), i.e., whether the coefficient β_2 in a linear regression $E[\ln\theta_{\max} \mid \ln S_a, M] = \alpha + \beta_1 \cdot \ln S_a + \beta_2 \cdot M$ is zero or not. Therefore, showing that β_2 is not statistically different from zero is a necessary but not sufficient condition to prove sufficiency.

6.16 Investigating the sufficiency of PGA as the intensity measure with respect to magnitude

The previous studies showed $S_a(T_{FM})$ to be (at least linear first order) sufficient with respect to the ground motion characteristics, magnitude M, rupture distance R_{rup}, and the attenuation epsilon, ε. What happens if the intensity measure is not sufficient with respect to the ground motion characteristic variables? The peak ground acceleration (PGA) is commonly perceived as an "insufficient" intensity measure for moderate to long-period buildings. In this section the sufficiency of PGA as the candidate intensity measure is studied with respect to M, R_{rup}, and ε, for the LA 20 building.

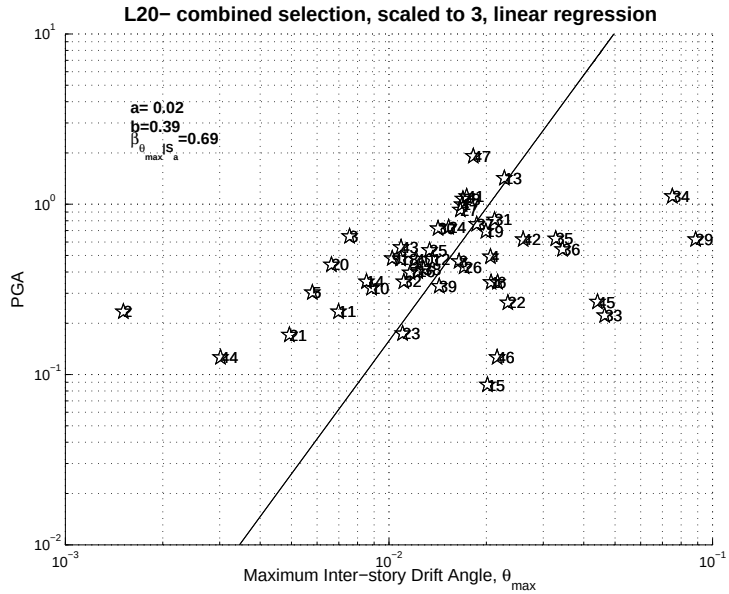

Figure 6-22 - The "original" regression of the displacement-based response on PGA, LA 20 building, the records scaled by a factor of 3.

For reasons discussed in Sections 6.11 and 6.12, the moment magnitude is the most likely ground motion variable to affect the displacement-based response. Hence, it would be interesting to investigate the sufficiency of PGA with respect to magnitude. The displacement-based response of the LA 20 structure to the records scaled by a factor of 3 are plotted versus PGA in Figure 6-22. The "original" regression prediction of the response as a function of PGA (i.e., the fitted line) is also plotted in the figure. The residual-residual plot for magnitude as a second regression variable is illustrated in Figure 6-23.

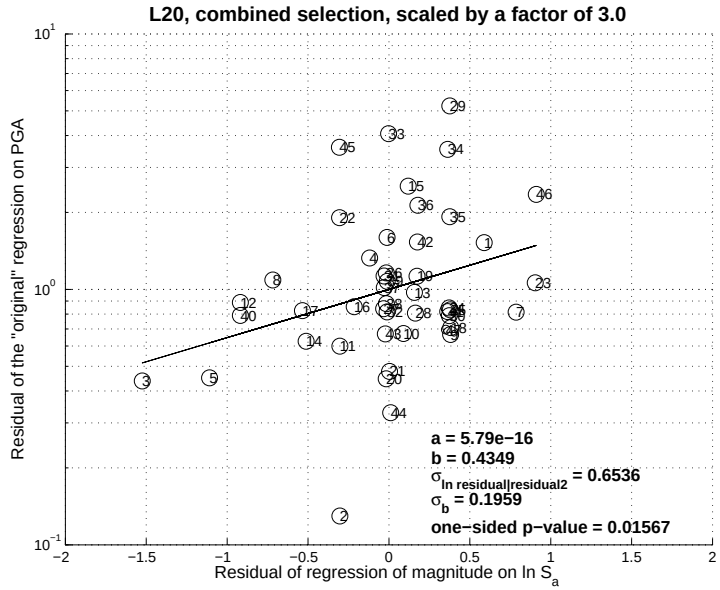

Figure 6-23 - The residual-residual plot for magnitude as a second regression variable, LA 20 structure, "combined" record set scaled by a factor of 3.

It can be observed that the residuals of the "original" regression of $\ln\theta_{\max}$ on PGA demonstrate a positive trend with respect to the residuals of the regression of magnitude on PGA. As discussed before in Section 6.11, large-magnitude events have a relatively strong frequency content in the short frequency range. Hence, the positive trend observed in Figure 6-23 seems reasonable. The trend observed in the residual-residual plot in Figure 6-23 is quite strong as indicated by the slope parameter b=0.435. Also, the *p-value*=0.0157 suggests that the observed trend is also quite significant. However, the small reduction in the "sigma" (i.e., 0.65 in the residual-residual regression versus 0.69 of the "original" regression) implies that M is not very helpful in increasing the efficiency, compared to PGA alone. Therefore, one may conclude that PGA in this case is not sufficient with respect to magnitude, but the addition of magnitude as a second regression variable may not (practically) increase the efficiency.

6.17 Adjusting for possible dependencies using weighted regression

It was concluded in the previous section that PGA is not sufficient with respect to the ground motion magnitude. Using a weighted regression scheme (Weisberg, 1985) may help in reducing the dependence of the residuals (of the "original" regression on PGA) on magnitude. Shome (1999) implemented the weighted regression scheme in order to take into account the effect of the SMF shape factor in predicting the response.

It should be recalled that regression analysis works by minimizing the sum of the squared errors (residuals) between the observed drift and the predicted drift. The weighted regression scheme weights each error term (residual) proportional to its corresponding variance. A similar weighting scheme is implemented in this section in order to adjust the residuals (of the "original" regression of $\ln\theta\max$ on PGA) with regard to their dependence on magnitude

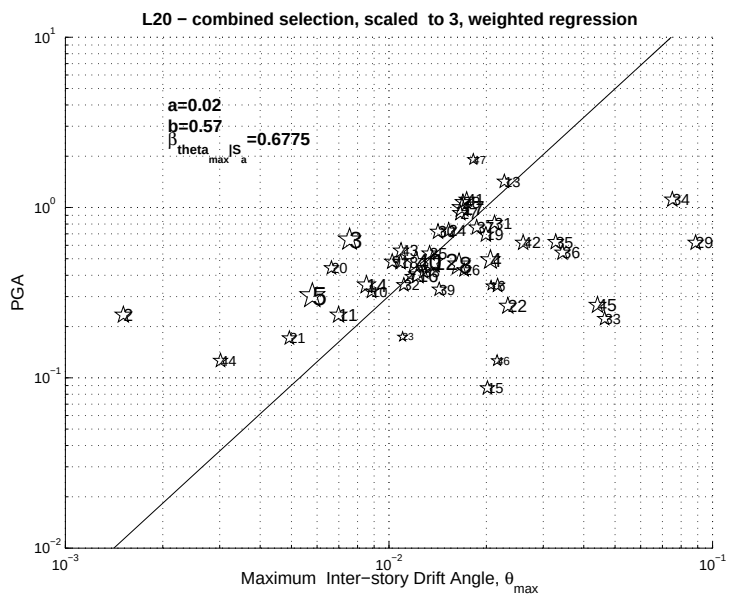

Figure 6-24 - The weighted regression of the displacement-based response on PGA, LA 20 structure, the "combined" set of record scaled by a factor of 3.

It can be argued that the variance of each error term and hence the corresponding weight may be positively related (ideally, proportional) to the following ratio:

$$w_i \propto \frac{p_{M|PGA}(m_i \mid x)_{disaggregation}}{p_{M|PGA}(m_i \mid x)_{data}} \qquad (6\text{-}13)$$

where $p_{M|PGA}(m \mid x)$ is the is the fraction of the ground motions with magnitude m for a given PGA equal to x. For the suite of record used in this chapter, $p_{M|PGA}(m_i \mid x)_{data}$ is equal to $1/N_T$ (i.e., no two records in this set have the exact same magnitude and PGA), where N_T is the total number of records. $p_{M|PGA}(m_i \mid x)_{disaggregation}$ is the fraction of records with magnitude m_i for a given PGA equal to x, estimated from the disaggregation of hazard for a PGA equal to x (see Bazzurro and Cornell, 1997). This weighted regression scheme is applied to the displacement-

based response of the 20-story structure to the "combined" set of records scaled by a factor of 3. Figure 6-24 illustrates the resulting weighted regression prediction plotted against the same data points in Figure 6-22, plotted by stars with areas proportional to the corresponding weighting factor for the residuals.

Comparing the weighted regression parameters in Figure 6-24 to those of the "original" regression in Figure 6-22, it can be observed that the "sigma" is somewhat reduced from 0.69 to 0.6775, and also the b-value is increased from 0.39 to 0.57. In order to see how the weighting affects the sufficiency with respect to magnitude, the weighted residual-residual plot for magnitude is plotted in Figure 6-25. It should be noted that the residual-residual regression line in Figure 6-25 has a non-zero intercept. This is because the weighted residuals have a non-zero expected value. Also it can be observed that in general the smaller residuals have received larger weights (judging by the radii of the circles).

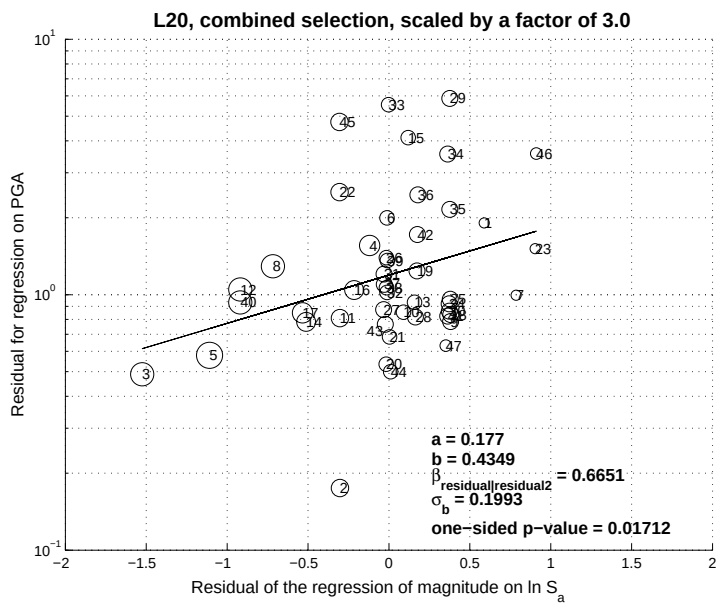

Figure 6-25 - The weighted residual-residual plot for magnitude, LA 20 structure, the "combined" record set scaled by a factor of 3.

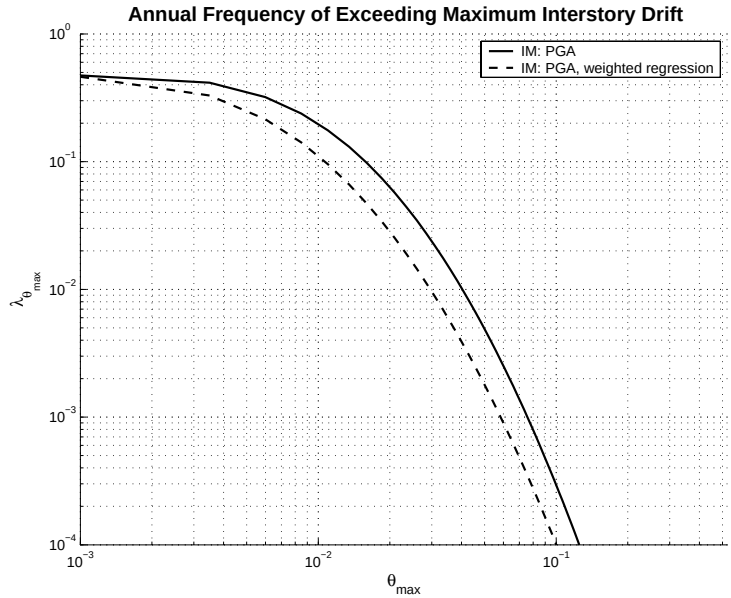

Figure 6-26 -The hazard curves for the displacement-based response with PGA as the intensity measure. The hazard curve in dashed lines is based on weighted regression.

However, it would be interesting to study how the probabilistic assessments for the displacement-based response are going to be affected by the weighed regression scheme. Figure 6-26 illustrates the hazard curves for displacement-based response with PGA as the intensity measure. The hazard curves are calculated by numerical integration of Equation 6-14 below (Similar to Equation 4-5-a with spectral acceleration as the IM):

$$\lambda_{\theta_{\max}}(y) = \int_x P[\theta_{\max} > y \mid PGA = x] \cdot \left| d\lambda_{PGA}(x) \right| \qquad (6\text{-}14)$$

where $\lambda(.)$ is the hazard function or in more detail, the mean annual probability of exceedance. The term $P[\theta_{\max} > y \mid PGA = x]$ or the probability of exceeding the displacement-based response value y for a given value of PGA can be calculated by implementing the regression parameters discussed previously assuming that the conditional probability distribution for the displacement-based response is lognormal. The solid line in Figure 6-26 is based on the "original" regression parameters from Figure 6-22 and the dashed line is based on the "weighted" regression parameters from Figure 6-24. The term $\lambda_{PGA}(x)$ or the hazard function for PGA can be estimated by the site-specific PGA hazard curve for a site in LA based on Abrahamson and Silva's attenuation law for horizontal motion on soil (see Abrahamson and Silva 1997), and calculated

using a probabilistic seismic hazard software developed by Norman Abrahamson (see Abrahamson 2001, hazard code version 30).

In order to be able to judge if the weighted regression is helpful in adjusting for the dependence on magnitude, the hazard curve for the displacement-based response has been calculated with the pair [PGA, M] as the intensity measure. Similar to Section 6.15, the hazard curve can be calculated by expanding the term $P[\theta_{\max} > y \mid PGA = x]$ in the expression for the hazard curve in Equation 6-14 with respect to magnitude (see Luco, 2001):

$$\lambda_{\theta_{\max}}(y) = \sum_i \int_x P[\theta_{\max} > y | PGA = x, M = m_i] \cdot p_{M|PGA}(m_i|x) \cdot \left| d\lambda_{PGA}(x) \right| \tag{6-15}$$

In a similar way, the term $P[\theta_{\max} > y \mid PGA = x, M = m_i]$ can be calculated by implementing the regression parameters for the multi-variable regression of the displacement-based response on PGA and M. The parameters for this regression are outlined in Table 6-7. Also the term $p_{M|PGA}(m_i \mid x)$ can be estimated from the results of the disaggregation of hazard for a PGA equal to x.

Regression on PGA and M	a	b_{PGA}	b_M	$\sigma_{\ln \theta_{\max} \mid PGA, M}$
scaled by 3	0.0012	0.376	0.4349	0.6536

Table 6-7 – The results of the linear multi-variable regression of $\ln \theta_{\max}$ on $\ln PGA$ and M for the case where the ground motion accelerations are scaled by a factor 3, LA 20 story building

Figure 6-27 illustrates the hazard curve calculated from Equation 6-15 together with the hazard curve shown in Figure 6-26. The thick line represents the hazard curve using the pair [PGA, M] as the intensity measure, the thin line represents the hazard curve using PGA as the intensity measure, and the dashed line represents the hazard curve using PGA as the intensity measure but adjusting for the dependence on magnitude by weighted regression. It can be observed that the hazard curve calculated using the weighted regression is almost identical to the one calculated using the pair [PGA, M] as the intensity measure. This indicates that the weighting scheme is effective for taking into account the magnitude dependence in the prediction of hazard for the displacement-based response.

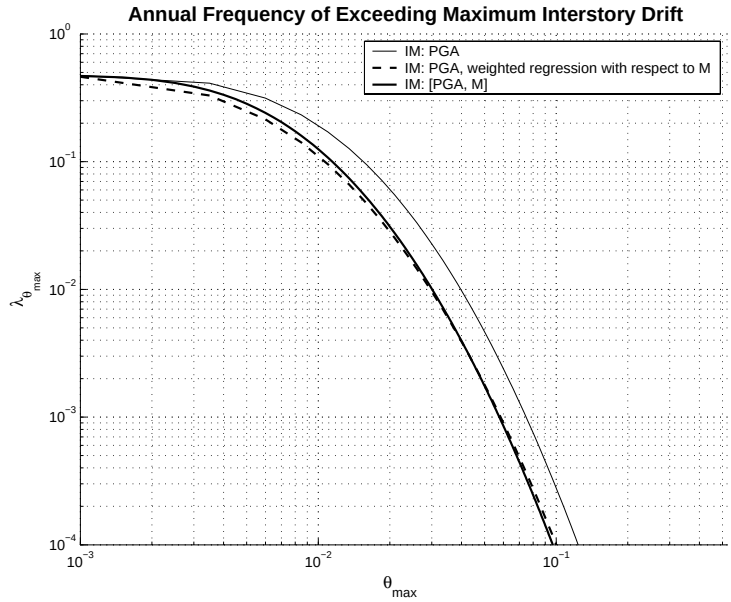

Figure 6-27 - The hazard curve for the displacement-based response with the pair [PGA,M] as the intensity measure (thick line) compared to the curves in Figure 6-26.

6.18 Summary and conclusions

It is argued that, theoretically speaking, careful record selection is not essential if the candidate intensity measure (IM) is demonstrated to be "sufficient" with respect to the ground motion characteristic variables. "Sufficiency" (see Luco and Cornell, 2001) is a probabilistic criterion for a preferred IM, in which the structural (displacement-based) response for a given IM level is conditionally statistically independent of the ground motion characteristics variables. A first-order approximation to the sufficiency criterion states that the conditional expected value of the structural response for a given intensity level is conditionally statistically independent of the ground motion characteristic variables. A suite of linear regressions was used as a statistical tool for investigating the "first-order" sufficiency of the candidate IM. In the cases where the "first-order" sufficiency for the candidate IM could not be established, a weighted linear regression scheme based on the results of the seismic hazard disaggregation with respect to the ground motion characteristic variable(s) was implemented in order to adjust for the observed dependencies.

In this chapter, the spectral acceleration at the first-mode frequency (FMF) was selected as the candidate IM. Also the maximum inter-story drift angle $\theta_{\max}$ represented the displacement-based

structural response parameter. A suite of (more-or-less arbitrarily selected) ground motion recordings on stiff soil was used in this chapter for dynamic time-history analyses. In this chapter, the non-linear dynamic displacement-based responses of two extreme cases of short-period and long-period structural systems were studied. The short-period system is a generic SDOF bi-linear model with T=0.1; and the long period system is a 20-story moment-resisting steel frame structure (LA 20 structure) with $T_1 = 3.98$. It was demonstrated for both structural systems that the FMF spectral acceleration is "effectively" sufficient with respect to ground motion characteristic variables, magnitude M, distance R_{rup}, and the "epsilon" of the attenuation relation. It was also demonstrated that the structural response for a given FMF spectral acceleration is (strongly) dependent on the shape of the elastic acceleration spectrum. The spectral shape factor, defined as the spectral acceleration at a period T normalized by FMF spectral acceleration, was the parameter used to represent the shape of the spectrum. For the high-frequency bi-linear SDOF system, the response was demonstrated to be positively related to the spectral shape factors at period longer than the FMF. This observation could be explained by the elongation of the effective period in the high ductility region. For the long-period 20-story structure, the response was shown to be positively related to the spectral shape factors at shorter periods close to that of the second-mode frequency (SMF). This confirmed the a priori expectation that the response of the tall long-period moment-resisting frame be dependent on the higher modes.

Among the ground motion characteristic variables, the moment magnitude is generally perceived to be the most likely one to affect the structural response once it is conditioned on FMF spectral acceleration. The validity of such perception is tested in this chapter by studying the correlation between the spectral shape factor and magnitude based on the attenuation relation predictions and also on the suite of records used in this chapter. It is demonstrated that high-frequency spectral shape factors (i.e., periods close to or smaller than T_{SM}) are negatively correlated with magnitude. This could be explained by the fact that the small-magnitude events are (physically) less capable of generating long-period (low-frequency) waves. This together with the observed positive correlation between the response of the long-period 20-story structure and the high frequency spectral shape factors leads one to expect that the structural response will be negatively correlated with magnitude. This seems to contradict previous observations indicating that the response for a given FMF spectral acceleration does not display a statistically significant dependence on magnitude. However, a closer look at the relations between magnitude and spectral shape factor and between the response and the shape factor indicates that there is

considerable uncertainty (i.e., uncertainty due to record-to-record variability) in these relations (judged by the large *p-values*). On the other hand, the weak negative correlation observed between the (conditional) response and magnitude is categorized as statistically insignificant due to the large uncertainties involved in the predictions.

Similar observations have been made for different ductility levels. The yield strength level for the high-frequency bi-linear SDOF system is adjusted so that different levels of ductility in the response are achieved. It was demonstrated, based on the response of the SDOF system with modified yield strength, that the FMF spectral acceleration is "effectively" sufficient with respect to ground motion characteristic variables. For the 20-story long-period structure the ground motion records are scaled by a factor of 3 in order to achieve a higher level of ductility in the response (the response to the un-scaled records was effectively in the linear range). Based on the response of the 20-story structure to the suite of records scaled by a factor 3, it was again established that FMF spectral acceleration is sufficient with respect to ground motion characteristic variables.

In order to study a case in which the candidate IM is not sufficient with respect to ground motion characteristic variables, the peak ground acceleration (PGA) was adopted as the candidate IM. Based on the response of the 20-story structure to the suite of records scaled by a factor 3, it was observed that PGA is not sufficient with respect to ground motion magnitude. This again indicated that the uncertainty due to record-to-record variability in the correlation between the conditional response and magnitude very large and hence the observed dependence is not very strong. A weighted regression scheme based on the results of the disaggregation of the hazard for PGA with respect to magnitude was used to adjust for the dependence on magnitude. The estimated hazard curve for the displacement-based response based on weighted regression was very close to the one derived by adopting the pair [PGA, M] as the intensity measure. Hence, it was concluded that the weighted regression enhances the hazard estimations for the displacement-based response of the 20-story structure.

6.18.1 Limitations

It is important to note that the observations made in this chapter are subject to certain limitations. The suite of records used in this chapter excludes near-source records that usually have more propensity for causing near-source effects such as directivity in the response. Also the observations made for the long-period structure are specific to the 20-story structure studied in

this chapter. The ground motions were scaled in some cases in order to achieve higher degrees of ductility. It was implicitly assumed in doing so the scaled ground motions are able to affect the response more-or-less (more accurate?) in the same way as the ground motions that are (naturally) stronger. This is supported by the demonstrated sufficiency which implies that larger M and ε or smaller R_{rup} (which would imply strong records) would not affect the responses (given spectral acceleration) Finally the sufficiency of the FMF spectral acceleration was established using a suite of simple mono-variable regressions; this ignored possible correlations between the ground motion characteristic variables. A more thorough approach would implement multi-variable regression in order to take into account possible cross-correlations between ground motion characteristic variables.

6.19 Acknowledgments

The authors would like to acknowledge the Pacific Earthquake Engineering Research Center, PEER, funded by the U.S. National Science Foundation (Project No. 3202000). They would also like to thank Dr. Nicolas Luco for providing the MDOF structural model.